Large-Scale Atmospheric Circulation Variability and its Impacts on the Nordic Seas Ocean Climate - a Review

Tore Furevik[1]

Geophysical Institute, University of Bergen, Norway

J. Even Ø. Nilsen

Nansen Environmental and Remote Sensing Center, Bergen, Norway

CITATION: Furevik, T. and J.E.Ø. Nilsen (2005). Large-Scale Atmospheric Circulation Variability and its Impacts on the Nordic Seas Ocean Climate - a Review, in Drange et al. (eds.), *The Nordic Seas: An Integrated Perspective*, *Geophysical Monograph Series* **158**, AGU

The large-scale atmospheric circulation and its impacts on the Nordic Seas ocean climate are reviewed. The dominant factors for the atmospheric variability are the Icelandic low and the Azores high, determining the strength of the westerlies. From the '60s to the '90s, the atmospheric circulation shifted from record weak to record strong westerlies, and the storm tracks moved further northeast into the Nordic Seas. The reasons for this shift have most likely been forcing from the tropical ocean in combination with internal processes in the atmosphere. Associated with this low-frequency shift are changes in the atmospheric momentum, heat, and freshwater forcing of the ocean. Both local processes and advective anomalies have played active roles in the substantial changes observed in the Nordic Seas' circulation and hydrography over the same period. These include a reduction in the deep-water formation, a warming of the water going into the Arctic, and a freshening and probable reduction of the overflow water.

The strengthening of the westerlies is concurrent in time with a strong increase in global mean temperatures, and we speculate that the changes in the atmospheric circulation are tied to the increased greenhouse gas forcing through a variety of forcing mechanisms. If so, the observed changes in the Nordic Seas ocean climate are likely to be amplified, and our perceptions of what is normal oceanic conditions will be further challenged in the years to come.

1. INTRODUCTION

By having the North Atlantic Ocean to the south, and the Arctic Ocean to the North, the Nordic Seas act as a buffer zone between the warm, saline Atlantic Water (AW), and the cold, fresh Polar Water (PW). These two water masses outline the main features of the surface water in the Nordic Seas as AW occupies the southern and eastern part of the basin and PW the northern and western part. A detailed description of the water masses, their flow patterns and water modifications, as well as the topographical features within the Nordic Seas is given by *Hansen and Østerhus* [2000] and *Blindheim and Østerhus* [this volume]. Only a brief outline will therefore be given here. The focus will be on the

features of the surface flows that are important for the discussion of the atmospheric impacts on the oceanic circulation.

The major opening to the Arctic Ocean is the Fram Strait, but also the shelf areas of the Barents Sea provide important pathways between the Nordic Seas and the Arctic Ocean (Figure 1). The main source for PW to the area is the East Greenland Current (EGC) which flows southward from the Fram Strait and along the western margin of the basin, branching off PW into both the Greenland and Iceland Seas on its way.

Figure 1

The Greenland–Scotland Ridge (GSR) forms the natural border to the Atlantic Ocean and provides three gateways for the exchange of water masses between the basins: The Denmark Strait between Greenland and Iceland, the Iceland–Faroe Ridge (IFR), and the Faroe–Shetland Channel (FSC). Further to the south, the North Atlantic Current (NAC) starts off as a western boundary current originating from the Gulf Stream [*Bower et al.*, 2000; *Carr and Rossby*, 2001]. The NAC passes over the Charlie Gibbs Fracture Zone (CGFZ) and spreads in different paths towards to the three openings of the GSR.

The AW passing over the IFR forms the Iceland Faroe Front against the PW in the central Nordic Seas and turns eastward as the Faroe Current and subsequently as the western branch of the Norwegian Atlantic Current (NwAC) [*Mork and Blindheim*, 2000; *Orvik et al.*, 2001]. Through the FSC the major source of AW is the slope current over the Scottish Slope, originating off the southwestern European coast [*Hansen and Østerhus*, 2000] and continuing northwards along the Norwegian Continental Shelfbreak as the eastern branch of the NwAC [*Mork and Blindheim*, 2000; *Orvik et al.*, 2001].

Within the Nordic Seas, the strongly topographically steered eastern branch of the NwAC follows the continental slope to the Barents Sea and Fram Strait, and provides the source for the AW in the Arctic Ocean. The fate of the more meandering western branch is more disputed. Drifter measurements indicate that the flow continues into the Fram Strait [*Orvik and Niiler*, 2002], where probably most of the water recirculates south [see *Quadfasel et al.*, 1987; *Gascard et al.*, 1988].

During recent years there has been an increased focus on the many atmospheric and oceanic processes taking place in the Nordic Seas and the Arctic Ocean. There are at least four good reasons for this: Firstly, since the '60s the westerlies have strengthened, resulting in dry, cold winters in southern Europe, and wet, mild winters in northern Europe [*Hurrell*, 1995]. Secondly, during the same period the deep-water formation in the Greenland Sea has been strongly reduced, and the export of dense water to the North Atlantic seems to have weakened [*Dickson et al.*, 1996; *Hansen et al.*, 2001]. Thirdly, the Arctic Ocean has become warmer [*Carmack et al.*, 1995; *Grotefendt et al.*, 1998], and the Northern Hemisphere sea-ice cover has decreased both in extent [*Johannessen et al.*, 1999, 2004] and thickness [*Rothrock et al.*, 1999, 2003]. Fourthly, the surface and intermediate water of the Nordic Seas, the overflow water, and the deep water of the North Atlantic have become fresher [*Blindheim et al.*, 2000; *Dickson et al.*, 2002; *Curry et al.*, 2003].

The aim of this paper is to give a review of the current knowledge of the large-scale atmospheric circulation variability over the North Atlantic, and of the role of the atmospheric forcing on the Nordic Seas ocean climate.

In Section 2 the large-scale atmospheric flow over the North Atlantic and Arctic is discussed. Focus is on the most prominent mode of sea-level pressure (SLP) variability, the North Atlantic Oscillation (NAO). The recent temporal and spatial changes in the NAO are reviewed, and proposed forcing mechanisms discussed. The variations in the atmosphere-ocean heat and momentum fluxes associated with changes in the NAO is studied in Section 3, and in Section 4 theoretical effects of the anomalous atmospheric forcing on the ocean properties in the Nordic Seas are considered. In Section 5 recent observations of the variability and trends in the ocean climate are discussed in light of anomalous forcing, and in Section 6 possible links between the changes observed in the Nordic Seas and global warming are discussed. The review is summarized and concluded in Section 7.

2. LARGE-SCALE ATMOSPHERIC CIRCULATION

The winter-mean (Dec–Mar) SLP field over the Northern Hemisphere is dominated by high pressure cells over the continents and subtropical oceans, and low pressure cells over the subpolar Atlantic and Pacific Oceans (Figure 2a). A weaker SLP maximum is the Beaufort high situated over the perennial sea-ice cover in the Canadian Basin in the western part of the Arctic Ocean. Maximum interannual variability in winter-mean SLP is found over the subpolar lows in the Atlantic and Pacific, where year-to-year standard deviation exceeds 9 hPa (Figure 2b). Also the Siberian high experiences enhanced interannual variability.

Figure 2

2.1. Station Based Indices for the Atmospheric Variability

The strength of the westerlies between the North Atlantic subtropical high and subpolar low, known as the Azores high and the Icelandic low respectively, has a profound impact on the climate of the North European region, as well as on a wide range of physical, ecological, and social parameters in the Atlantic sector [see *Marshall et al.*, 2001b; *Hurrell et al.*, 2003, and references therein]. As a consequence, many scientists have tried to find useful indices for describing the strength of the westerlies and thus proxies for the climate of Europe. The best known are the NAO indices based on the SLP differences between Lisbon, Portugal and Stykkisholmur, Iceland [*Hurrell*, 1995], or between Gibraltar and Stykkisholmur [*Jones et al.*, 1997], succeeding the Azores-Iceland indices first used by *Bjerknes* [1962] and later *Rogers* [1984]. Other indices have been constructed as proxies for more local- or regional- scale phenomena, for instance the SLP difference across Fram Strait for the sea-ice export [e.g. *Vinje*, 2001; *Widell et al.*, 2003] or across the Barents Sea Opening to explain the inflow of AW [*Bengtson et al.*, 2004].

If the Gibraltar and Stykkisholmur SLP data are grouped into each individual month, distinct annual cycles in both monthly means and monthly variances emerge (Figure 3). At Stykkisholmur, minimum SLP is in January and maximum in May, while Gibraltar is in opposite phase, having maximum in January and minimum in May. As a consequence, the average mean SLP difference between the two stations varies from only 2.9 hPa in May to 23.6 hPa in January, illustrating the strong seasonal dependency of the westerlies. Also the interannual variability in SLP varies with month, with maximum standard deviation for the two stations' monthly means being in February (9.9 and 4.0 hPa) and minimum in July (3.7 and 0.9 hPa).

Figure 3

For the winter months December through March, the Gibraltar and Iceland stations used to construct the Jones index are anti-correlated also at interannual and interdecadal time scales, with correlations being between -0.65 and -0.55. From May to September correlations are small and not significant at the 95% confidence level. The main reason for this is that the mesoscale structures are smaller and less organized during summer compared to winter. As shown by *Portis et al.* [2001] the same is true for the Lisbon and Iceland station pair used in the Hurrell index, while the Azores and Iceland station pair used in the Rogers (Bjerknes) index show a significant anti-correlation throughout the year. As an alternative to the traditional index with fixed station pairs, *Portis et al.* [2001] proposed an index based on the SLP differences between the two geographical points having highest anti-correlation, giving an index better at capturing the north-south SLP gradient throughout the year.

The perhaps main reasons for the increasing interest in the NAO is the trend towards stronger westerlies that has occurred since the '60s, captured in both the *Hurrell* [1995] and *Jones et al.* [1997] indices (Figure 4a). A high (positive) NAO-index corresponds to a large-scale shift of atmospheric mass from the Icelandic low, Nordic Seas and Arctic Ocean region towards the Azores high (Figure 4b). Associated with a positive NAO-index, the Icelandic low extends more northeast into the Nordic Seas, where the changes in the SLP associated with a unit change in the NAO-index exceed 7 hPa. Over the Arctic Ocean, the corresponding changes range from 4 hPa near the Fram Strait to less than 1 hPa near the Bering Strait. Near the subtropical high, a unit change in the NAO-index corresponds to a 4 hPa change in SLP.

Figure 4

2.2. EOF-based Indices for the Atmospheric Variability

An alternative method for extracting useful indices for the strength of the large-scale atmospheric circulation is to apply an Empirical Orthogonal Function (EOF) analysis [e.g. *von Storch*, 1995]. Typically, a singular value decomposition method is used to construct the dominant modes of variability as load functions (EOF patterns) and associated time series (principal components). The idea is to find the patterns and associated time series that explains as much as possible of the variance in the data set, and if possible give a physical interpretation of these modes.

In Figure 5 the leading mode of the winter SLP anomalies is shown. The principal component defines the atmospheric index used throughout the paper, which for simplicity will be referred to as the NAO-index. In this analysis the EOF was calculated based on the December through March SLP data from the Atlantic sector only, in contrast to the November through April data from all longitudes and poleward of 20°N that were used by *Thompson and Wallace* [1998] to define their Arctic Oscillation index. As pointed out by *Deser* [2000], the EOF patterns are practically identical whether the circumpolar data or only the Atlantic sector is used. For the data used here, their associated principal components have a mutual correlation of 0.99.

Figure 5

The EOF pattern (Figure 5b) shows a tripole structure. For positive values of the principal component, SLP over the Arctic is lower, and SLP over the Azores high and the Aleutian low is higher than normal. This corresponds to stronger than average westerlies in the Atlantic sector, while the westerlies in the Pacific are actually reduced. The fact that the EOF is somehow annular in shape, but with strongest amplitudes in the Atlantic sector, is one of the causes for the discussion on whether this is an Arctic or annular mode [*Thompson and Wallace*, 1998, 2000], or if it is more physically correct to name it the North Atlantic Oscillation [*Hurrell*, 1995; *Deser*, 2000; *Ambaum et al.*, 2001].

The EOF pattern clearly resembles the pattern found by regressing the winter-mean SLP pressure on the two-pole Jones index (Figure 4), and is obviously a manifestation of the same feature. Nonetheless, some differences should be noted. The EOF pattern has weaker poles, but at the same time a wider domain of influence, most noticeably from the Barents Sea and east into the northern parts of Siberia, and to the south of the Bering Strait. Interestingly, most of the differences are found outside the Atlantic sector used to calculate the principal component, which may indicate teleconnectivity between these areas and areas within the Atlantic sector not captured by the two-pole index. The differences over the Atlantic sector is due to the fact that the regression on the two-pole index will maximize the variance explained at those two particular locations, while the regression onto the principal component will maximize the variance explained over the entire Atlantic sector, and thus give a somewhat weaker pattern over the Azores high and Icelandic low.

While the two-pole indices directly give the SLP gradient and thus measure the strength of the geostrophic flow between the station pairs, EOF-based indices are based on the statistical properties of the entire SLP field in the domain that is analyzed. For this reason the EOF-based indices more adequately represents the spatial domain of the mode of variability. The EOF-based indices should however be treated with care. Variability somewhere in the domain that is analyzed will influence the pattern in other areas of the domain, and vice versa. Thus, there remains a degree of subjectivity to the choice of size of the domain. Furthermore, adding new data to an existing time series will change the EOF pattern and thus the principal component associated with that mode. The result is that the entire EOF-based index will change as new data are added, and results may have to be recalculated.

2.3. Temporal Changes in the Large-Scale Circulation

Since *Hurrell* [1995] demonstrated the strong influence of the NAO on the European climate, there has been a huge growth in the scientific interest in the subject [see *Stephenson et al.*, 2003, for a historical review]. Due to the large impact of the large-scale atmospheric circulation on the climate in the North Atlantic region, much effort has been made to understand the causes for the NAO variability, with the ultimate goal to be able to predict the changes on seasonal to decadal time scales. A common method has been to use a statistical approach to observational data, and significant correlations are often found, for instance between the NAO and North Atlantic sea-surface properties [e.g. *Marshall*

et al., 2001b; *Czaja et al.*, 2003]. However, generally short and inhomogeneous observational records, the fact that the NAO strongly influences the state of the ocean (see Section 4), and the fact that both the ocean surface variability and the NAO may be driven by factors outside the Atlantic sector, all makes it extremely difficult to assess the predictability potential by statistical methods alone.

At present, there is no general consensus about the main driver of the large-scale atmospheric variability in the North Atlantic region. At least three good candidates have been proposed. Firstly, most of the variability in the NAO seems to arise from internal processes in the troposphere, where an important mechanism is by non-linear interactions between the time-mean flow and transient eddies causing an essentially white spectrum [*Thompson et al.*, 2003]. Further non-linearities or aggregation (combination of many short-lived processes) may in turn cause a reddening of the spectrum, and give rise to low-frequency behaviour similar to what has been observed in the recent decades [*Stephenson et al.*, 2000]. This is the most pessimistic explanation, as it gives no room for predictability of the NAO. However, while the bulk part of the monthly to interannual variability can be attributed to stochastic noise, it does not explain the increased variability and the strong upward trend in the last half of the 20th century [*Hurrell et al.*, 2004], nor does it explain the upward trend found in many climate projections for the 21st century [e.g. *Fyfe et al.*, 1999]. A comparison of the observed trend in the NAO with output from 7 different unforced climate models, where the observed trend was outside the most extremes of the natural variability ranges simulated by the models, led *Gillett et al.* [2003] to conclude that either all the models had deficiencies in the low frequency range, or the observed trend can only be explained by external forcing. And as many of the climate models in control simulations do a fairly good job in reproducing both the spatial pattern and the strength of the interannual variability in the large-scale circulation [e.g. *Fyfe et al.*, 1999; *Stephenson and Pavan*, 2003; *Furevik et al.*, 2003], the latter is therefore a plausible interpretation.

Secondly, observations and reanalysis data have shown that changes in the large scale circulation may start in the stratosphere, and gradually propagate downward into the troposphere [*Baldwin and Dunkerton*, 1999; *Baldwin et al.*, 2003; *Thompson et al.*, 2003]. The mechanisms are still not properly understood, but may involve stratospheric refraction of upward propagating gravity waves in the troposphere [*Ambaum and Hoskins*, 2002]. Despite the lack of solid evidence, this scenario is nevertheless intriguing owing to its large potential for extended weather forecast [*Baldwin et al.*, 2003]. Forcing from the stratosphere has also been suggested as a possible explanation for the trend towards strengthened westerlies in the latter part of the 20th century, either due to ozone depletion in the stratosphere and associated cooling over the polar regions [e.g. *Bengtsson et al.*, 1999; *Kindem and Christiansen*, 2001], or greenhouse gas forcing warming the troposphere and cooling the stratosphere [*Shindell et al.*, 1999], thus increasing the north-south temperature gradient near the tropopause [see review by *Gillett et al.*, 2003].

Thirdly, the most studied candidate for imposing low-frequency variability to the atmosphere, is the ocean. The traditional approach has been to search for a statistical relationship between the underlying Atlantic sea-surface temperature (SST) and the SLP variability. An early attempt was made by *Bjerknes* [1964], who concluded that short-term variations in the SSTs were associated with local forcing from the atmosphere, while longer-term variations involved changes in the oceanic circulation. He further proposed that on long time scales, a change in the oceanic heat transport would be compensated by an opposite-sign change in the atmospheric heat transport. Using an atmospheric general circulation model (AGCM) forced with observed SST and sea-ice anomalies, *Rodwell et al.* [1999] reproduced most of the observed interannual and interdecadal variability in the NAO. Furthermore, when they forced the model with typical SST anomalies in the North Atlantic only, local changes in the atmosphere-ocean heat and freshwater fluxes were again found to give a thermal and geopotential structure in the atmosphere that resembled the NAO. Several other authors have found NAO-like responses to SST anomalies in the North Atlantic [e.g. *Sutton et al.*, 2000; *Marshall et al.*, 2001b; *Czaja et al.*, 2003]. However, ambiguities and the potential for predictability can be questioned as the areas where the atmosphere seems to be most sensitive to SST variability roughly coincide with the areas where the forcing from the NAO on the ocean has its maximum [*Hurrell et al.*, 2004]. A more robust

result seems to be the simulated response to sea-ice anomalies in the Labrador Sea, where an increased sea-ice cover leads to a weakening of the NAO [*Kvamstø et al.*, 2004]. Similar negative feedbacks between sea-ice and the NAO (a more positive NAO phase leads to more sea-ice in the Labrador Sea) have also been reported by other groups [e.g. *Alexander et al.*, 2004; *Magnusdottir et al.*, 2004].

Recognizing that half the area of the Earth is confined to the sector between 30°S and 30°N, and that the global-scale atmospheric circulation is driven by the convection in the tropics [e.g. *Gill*, 1982], other authors have turned their attention towards these latitudes. One suggested mechanism involves the cross-equatorial SST gradient, where co-varying fluctuation in the SSTs, the trade winds, and the rainfall is known to exist [*Nobre and Srukla*, 1996]. Changes in the tropical SST and rainfall patterns could lead to changes in the extra-tropical Atlantic through modulation of the strength of the Hadley circulation [e.g. *Sutton et al.*, 2000]. Using an AGCM forced with observed SSTs, *Hoerling et al.* [2001] reproduced half the observed trend in the NAO since 1950 and onward. Repeating the experiment with observed SSTs only in the tropics (30°S–30°N) and annual cycle in SST elsewhere, they essentially got the same results, thus excluding the extra-tropics as the source for the trend in the NAO. They further argued that the main source of the NAO trend lies in the Indian Ocean, and involves tropical rainfall and adiabatic heating, the drivers for the extra-tropical circulation. Their work is expanded in *Hurrell et al.* [2004] where four different AGCMs and a multi-model ensemble of 67 members is used. They show that the results obtained by *Hoerling et al.* [2001], including the trend in the NAO, the importance of the tropics, and in particular the SST and rainfall changes in the Indian Ocean, are reproducible using different models. In *Hoerling et al.* [2004] the physical mechanisms linking the Indian Ocean to the North Atlantic atmospheric variability were studied, using a series of idealized experiments where a 1°C temperature anomaly was suddenly switched on in the Indian Ocean. After less than a month, an anomalous circulation resembling the positive NAO pattern was obtained. Without being conclusive, the authors speculate that the response in the Atlantic is primarily eddy driven rather than driven by Rossby wave dispersion, and that adjustment of the local storm track is important.

To summarize, it seems that the NAO is an inherent mode in the atmosphere that a variety of different forcings regress onto. Thus, evidence of one forcing mechanism should not exclude the others. There are reasons to believe that the changes observed in the strength of the westerlies are non-linear combinations of stochastic noise, greenhouse gas forcing near the tropopause, forcing from the stratosphere, and forcing from the ocean, where evidence points to the Indian Ocean as a key area. Additional possible forcing mechanisms including tropospheric aerosols, volcanoes, and solar forcing have been discussed by *Gillett et al.* [2003].

2.4. Spatial Changes in the Large-Scale Circulation

Most of the literature about the NAO and its impacts assumes that the SLP pattern associated with the specific station-based NAO-index in use has been stationary in time. This is, however, not the case. Among the first to observe that the correlation between the NAO and some measured or modeled quantity may break down due to changes in the spatial pattern of the NAO were *Hilmer and Jung* [2000]. In their study the NAO was compared with modeled sea-ice export through the Fram Strait. While they found a high correlation in the '80s and '90s, no significant correlations were found prior to this period.

Comparing the year-to-year variability in SLP between the first and latter part of the NCEP/NCAR reanalysis period (Figure 6a,b), it is evident that the variability has decreased to the west of Iceland, while it has slightly increased in the Nordic Seas, Barents Sea, and over the Eurasian Basin. The changes become even more pronounced when the leading modes of variability are calculated. Associated with an increase in the NAO-index, there is an SLP decrease in the Norwegian and Barents Seas from the first to the latter period, and an increase near the Azores high and Aleutian low (Figure 6c,d). The main consequence of this shift is that the NAO pattern becomes more zonal in the vicinity of the GSR, and more meridional in the Fram Strait. Another interesting feature is the strengthening of the Pacific variability associated with the NAO, in sharp contrast to the earliest reanalysis period.

Figure 6

The reason for the apparent eastward shift in the NAO pattern is at present not clear. Sensitivity

studies with atmospheric models have suggested that the position of the northern centre of action may be connected to the strength of the NAO. Low index values correspond to a westward displacement from the mean position, and high-index values to an eastward displacement [*Peterson et al.*, 2002; *Cassou et al.*, 2004]. Other model simulations suggest that the eastward shift may be linked to increased concentration of atmospheric CO_2 content. This was first pointed out by *Ulbrich and Christoph* [1999], but seems to be a tendency in most models participating in the second phase of the Coupled Model Intercomparison Project (CMIP2), as shown in a recent paper by *Kuzmina et al.* [2004].

3. Atmosphere-Ocean Flux Anomalies

Associated with variability in the large-scale atmospheric circulation, there will be anomalies in the exchanges of momentum, heat, and freshwater between the atmosphere and the ocean. In this section the NCEP/NCAR reanalysis data [*Kalnay et al.*, 1996] are used to quantify these anomalies in terms of absolute values and deviations from the mean. Although the NCEP/NCAR data assimilation system has been kept unchanged over the reanalysis period, artificial trends or jumps may still exist in the data due to changes in the observational systems. The two major changes were the establishment of the upper-air data observational network from 1948 to the International Geophysical Year in 1957, and the introduction of satellite data in 1979 [*Kistler et al.*, 2001]. The gridded variables provided by NCEP/NCAR are divided into three classes, depending on how much they are influenced by the available observations [*Kalnay et al.*, 1996]. While output such as air temperature, pressure, and wind components are strongly constrained by the observations, and therefore considered to be the most reliable products, the surface heat and freshwater fluxes are determined by the model system, and should therefore be used with more caution.

Although the NCEP/NCAR flux data may be strongly biased in certain areas [e.g. *Serreze and Hurst*, 2000; *Josey*, 2001], the interannual variability tends to be better correlated with independent observations [*Kistler et al.*, 2001]. Thus, using the reanalysis data in a qualitative more than quantitatively fashion, and focus on the low-frequency impacts of the NAO, we are confident that the main results of this section are trustworthy and not due to artificial trends in the reanalysis data.

3.1. Momentum Fluxes

The winter-mean (vectorial) wind field over the Nordic Seas is dominated by the Icelandic low, giving southwesterlies over the northeastern North Atlantic, along the coast of Norway, and in the southern part of the Barents Sea (Figure 7a). Along the east coast of Greenland, northerlies dominate. The surface wind speeds for the Nordic Seas (Figure 7b) are 9–10 ms^{-1}, with maximum in the area of weakest winter-mean winds, which is along the path of the lows [see *Sorteberg et al.*, this volume].

Figure 7

When the wind is regressed on the NAO-index, an increase in the index is seen to be associated with strengthened southwesterly airflow towards northern Europe. Associated with a unit increase in the index, there is a more than 3 ms^{-1} increase in the westerly winds in the northeastern North Atlantic, and 1–2 ms^{-1} increase in the eastern part of the Nordic Seas. The impacts on the winds in the Barents Sea, Fram Strait, and along the east coast of Greenland are small.

The NAO impact on the local wind speed is much smaller than the changes in the monthly-mean wind, and only reaches 1 ms^{-1}. Maximum is found northwest of Scotland and off the west coast of Norway. As demonstrated by *Vikebø et al.* [2003], this is also the area with the largest increase in extreme wind events throughout the reanalysis period (they defined an extreme wind event by the criteria that the six-hourly mean wind speed at a location should exceed twice the mean wind speed in that area).

The monthly-mean wind stress reaches 0.3 Nm^{-2} in the Denmark Strait and typically 0.1 Nm^{-2} west of Scotland and along the coast of Norway (Figure 8). Associated with a unit increase in the NAO-index, an increase of 0.05–0.1 Nm^{-2} is found in the northeastern part of the North Atlantic and in the southeastern part of the Nordic Seas. Less increase in wind stress is found along the eastern coast of Greenland.

Figure 8

3.2. Heat Fluxes

From the NCEP/NCAR data we have extracted the heat fluxes divided into sensible, latent, short-wave, and long-wave radiative heat fluxes. The sensible and latent parts are shown in Figure 9a,b. Over the central parts of the Nordic Seas, the reanalysis has a sensible heat loss from the ocean ranging from 40 to 80 Wm^{-2} during winter, with maximum exceeding 100 Wm^{-2} along the marginal ice zone in the Barents Sea, Fram Strait, and Greenland Sea. Over the sea-ice there is a downward flux of sensible heat, as the surface of the ice is generally colder than the atmosphere due to the long-wave radiation from the sea ice. The latent heat flux is the larger component in the winter heat budget, with typical values of 80–100 Wm^{-2} over most of the Nordic Seas. Maximum is over the pathways of the warm flow of AW within the Nordic Seas (Figure 1) which also is where the winds are strongest (Figure 7b).

Figure 9

If the four atmosphere-ocean heat flux components are added, the net upward winter-mean heat flux is 160–180 Wm^{-2} over most of the region, with maximum oceanic heat flux exceeding 300 Wm^{-2} where the relatively warm water of the West Spitsbergen Current meets the cold Arctic air in the Fram Strait. Values between 200 and 300 Wm^{-2} are also found in most of the ice-free Barents Sea, which is the sub-basin within the Nordic Seas–Arctic Ocean system having the highest annual-mean heat loss. In a comprehensive study, *Simonsen and Haugan* [1996] estimated that 50% of the total heat loss from the Nordic Seas occurs in the Barents Sea, in total 136 out of 242 TW. In comparison, they found that only 86 TW were lost from the Arctic Ocean.

The effect of the increased wind speeds associated with a more positive NAO (Figure 7d), is a strong increase in the heat loss in the northwestern North Atlantic (Figure 9d). Near the tip of Greenland, the NAO forced heat loss is more than 40 Wm^{-2}, which is a 20% change from the winter-mean of 200 Wm^{-2}. Both sensible and latent heat fluxes contribute to this. Maximum is found over the Labrador Sea [see also *Visbeck et al.*, 2003]. Over the Nordic Seas, the effect of a positive NAO phase is to reduce the heat loss to the atmosphere, typically of the order of 5–10 Wm^{-2}. An exception is in the marginal ice zone, where a retreat of the sea-ice cover associated with the NAO may locally more than double the heat loss to the atmosphere.

3.3. Freshwater Fluxes

According to the reanalysis data, typical evaporation rates over the Nordic Seas range from 1 mm day^{-1} near the ice covered regions, to 3 mm day^{-1} over the warm tongue of AW (Figure 10a). This can be compared to the precipitation rates of typically 3–5 mm day^{-1}, indicating a net freshwater supply to the ocean of 1–2 mm day^{-1}.

Figure 10

Associated with the NAO, there is more evaporation to the south and west of Iceland and along the marginal ice zone east of Greenland, and slightly less evaporation in the North Sea and in the Baltic Sea (Figure 10c). The NAO impact on the precipitation is much stronger, with close to 1 mm day^{-1} additional precipitation south of Iceland and along the coast of Norway associated with a unit increase in the NAO index (Figure 10d).

4. IMPACTS ON THE OCEAN CLIMATE

Large-scale changes in the atmosphere-ocean fluxes may impact the ocean climate through a variety of mechanisms and on a wide range of time scales, ranging from days to years. Locally, there will be a rapid response in sea-surface height, mixed layer depth, sea-surface temperature (SST), and sea-surface salinity (SSS) due to anomalies in the atmosphere-ocean momentum, heat, and freshwater fluxes. While anomalous momentum fluxes and divergences in the associated Ekman transports will change the sea-surface height and mixed layer depth directly, leading to barotropic and baroclinic adjustment processes, it will also have an indirect effect on the SST and SSS fields. Divergence of heat or freshwater by the Ekman transports, or diapycnal mixing with the water below the mixed layer will add extra terms to the energy and salt balance equations.

On the longer time scales, years to decades, the Nordic Seas' response to anomalous forcing can include advection of heat or freshwater anomalies from distant regions, changes in the flow speed or position due to changes in the baroclinic structure of the upper ocean, or changes in the abyssal circulation due to buoyancy forcing in the convective regions.

In the following sections, some of the responses of the large-scale atmospheric forcing on the ocean climate are discussed. For more thorough treatments of the various aspects of the subject, we refer to the papers by *Anderson and Gill* [1975], *Anderson and Killworth* [1977], *Willebrand et al.* [1980], and to the textbook by *Gill* [1982].

4.1. Ocean Circulation

The direct response of an anomalous wind stress $\boldsymbol{\tau}'$ acting on the ocean surface is to set up a transport in the upper waters given by

$$\mathbf{U}_{ek} = -\frac{1}{\rho_0 f}\mathbf{k} \times \boldsymbol{\tau}' \tag{1}$$

where $\mathbf{U}_{ek}$ is the so-called Ekman volume transport per unit length ($\mathrm{m^2 s^{-1}}$), ρ_0 is the mean density, f is the Coriolis parameter, and $\mathbf{k}$ is the vertical unit vector.

Associated with the mean wind stress over the Nordic Seas (see Figure 8), the Ekman transports show a diverging field over the central Nordic Seas, with on-shore transports towards all surrounding land areas (Figure 11). Typical estimates for the transports are of the order of 1 $\mathrm{m^3 s^{-1}}$ through a section of 1 m width. Note that (1) is only valid for an atmospheric wind stress over an ice-free ocean. A sea-ice cover will significantly modify both the air-sea momentum exchanges and the associated Ekman transports, and the results for the ice-covered regions should therefore be used with caution.

Figure 11

As shown in Figure 8b, stronger than average westerlies are associated with an increased wind stress curl over the Nordic Seas, giving rise to strengthened Ekman transports. The region with strongest response is to the south of Iceland, where the Ekman transports (and wind stress) are nearly doubled during years when the NAO-index is one unit above average (Figure 11b).

If the wind stress was spatially uniform, the water below the mixed layer would not have been affected by the wind. However, when lateral boundaries are present or if the wind stress is spatially varying, the Ekman transports will be divergent. The result will be changes in the surface elevation and mixed layer depth, and a distortion of the pressure gradient throughout the water column, producing barotropic and baroclinic flow anomalies. We will first look at the effects of side boundaries.

When the wind stress has a component τ_s parallel to a coast, linear theory gives a constant growth rate for the surface elevation η and along-shore velocity u, given by

$$\eta = \frac{\tau_s}{\rho_0\sqrt{gH}} e^{-y/a} t \qquad \text{and} \qquad u = \frac{\tau_s}{\rho_0 H} e^{-y/a} t, \tag{2}$$

where g is the gravity, H is the water depth, $a = \sqrt{gH}/f$ is the Rossby radius, t is the time, and the y-axis is pointing outwards from the coast [e.g. *Gill*, 1982]. When bottom stress is included, the solutions will grow asymptotically towards equilibrium, having constant surface elevation and along-shore transports. Associated with an increase in the sea level near the coast, down-welling motion will occur in the water below the Ekman layer, changing the internal density structure in the fluid. Thus in addition to the sea-level response to the on-shore Ekman transport, leading to fast propagating coastally trapped barotropic waves, modifications of the internal pressure fields will lead to much longer adjustment time scales, and slower-propagating coastally trapped baroclinic waves with a typical speed of 1–2 $\mathrm{ms^{-1}}$.

In the open ocean, a spatial varying wind stress will force vertical motion known as Ekman pumping, where the strength of the vertical motion, w_{ek} is given by

$$w_{ek} = \frac{1}{\rho_0 f}\mathbf{k} \cdot \nabla \times \boldsymbol{\tau}'. \tag{3}$$

Calculations made for the Nordic Seas area are shown in Figure 12. The dominant long-term mean features are upwelling motion (positive Ekman pumping velocities) over most of the area, with values exceeding 40 cm per day in the western part. Only the northwestern corner of the Barents Sea, where the mean wind stress shows an anti-cyclonic pattern (see Figure 8a), has negative Ekman pumping. The response to the enhanced wind stress associated with the leading mode of variability is positive Ekman pumping anomalies in the western part of the basin, and negative anomalies to the southeast, where the anomalous westerly wind stress pattern is weakly anti-cyclonic (Figure 8b).

Figure 12

The response of the Ekman pumping in a flat-bottom ocean can be calculated using quasi-geostrophic theory [e.g. *Gill*, 1982]. An atmospheric low will introduce a positive wind stress curl to the ocean, where the barotropic response to the wind stress is a lowering of the sea level and the baroclinic response is a raising of the density surfaces below the low. Associated with the changes in the surface elevation and density distribution, there will be geostrophic currents increasing in strength with time. If the wind stress anomaly extends to the eastern rim of the ocean, or if the background flow field can carry the signal to the eastern boundary, barotropic and baroclinic planetary waves will be radiated into the interior of the ocean [*Anderson and Gill*, 1975]. Time scales will be of the order of days for the long, non-dispersive barotropic waves, and years for the baroclinic waves. After the wave front has passed, the flow becomes virtually stationary, and is given by the Sverdrup balance [*Sverdrup*, 1947], which is simply the conservation of potential vorticity given as

$$V_{sv} = \frac{1}{\rho_0 \beta} \mathbf{k} \cdot \nabla \times \boldsymbol{\tau}'. \tag{4}$$

Here V_{sv} is the meridional volume transport per unit length, and $\beta = df/dy$ is the rate of change of the Coriolis parameter with latitude.

The Sverdrup solution ignores the effects of topography and stratification. With bottom effects included, the lines of constant potential vorticity are f/H rather than f contours, and the effect of the Ekman pumping and vortex stretching will be to produce flow across f/H contours instead of meridional flow. With stratification also present, the influence of the topography will be reduced, and the Sverdrup theory therefore provides a good approximation to the large basin-scale circulation in the world oceans [e.g. *Gill*, 1982]. It should however be noted that the baroclinic adjustment time scale in the ocean makes the time to remove the influence of topography very long [*Anderson and Killworth*, 1977]. Thus, it is not a simple task to estimate how long an anomalous wind forcing must persist to set up a quasi-stationary Sverdrup circulation in a stratified flow over topography. By calculating the response of the North Atlantic to observed wind forcing, *Willebrand et al.* [1980] found little or no coherence between the atmospheric and the oceanic response at any frequency, which they attributed to the effect of topography. The usefulness of the Sverdrup solution for the weakly stratified, strongly topographically steered flows in the Nordic Seas areas may therefore be questioned.

4.2. Heat and Freshwater Divergence

In addition to the direct effect of the anomalous heat and freshwater fluxes imposed by the atmosphere, there may also be a local warming or freshening due to heat or freshwater divergences associated with the Ekman transports.

As shown by *Marshall et al.* [2001a], the Ekman induced contribution to the heat balance of the water column can be written

$$H_{ek} = c\rho_0 \mathbf{U}_{ek} \cdot \nabla T, \tag{5}$$

where c is the specific heat of water and T the temperature. Only the divergence in the heat transports are included in (5), any divergences in the Ekman induced mass transports are neglected. A positive contribution to the water temperatures is found where warm water is advected into areas with colder water (Figure 13). This is around the northern part of Great Britain and northeast towards the western coast of Norway, where AW is advected into areas dominated by the Norwegian Coastal Current (NwCC in Figure 1), and along the marginal ice zone along the east coast of Greenland. A

Figure 13

net cooling due to anomalous Ekman transports occurs in the northern North Atlantic and north of the Faroes, corresponding to a heat loss of more than 20 Wm^{-2}.

Following the same method as applied for the heat, the Ekman transport contribution to the fresh-water budget can be written

$$Q_{\mathrm{ek}} = -\rho_0 \mathbf{U}_{ek} \cdot \nabla S, \tag{6}$$

where S is here the dissolved salt per mass of sea water (i.e. the dimensionless salinity value divided by 1000). The reason for the minus sign is that an Ekman transport towards higher salinities will locally freshen the water column, and thus have the same effect as precipitation, which by definition is a negative freshwater flux. A positive contribution to the salinity in the water column is found where high-salinity water is advected into areas with lower salinities (Figure 14). These areas roughly coincide with the areas having a convergence of heat, that is to the west of Scotland, in the North Sea, along the coast of Norway, and along the east Greenland marginal ice zone. The Ekman effect here corresponds to an additional evaporation on the order of 0.1–0.2 mm day^{-1}, and it is thus small compared to the effects of evaporation and precipitation anomalies. The Ekman effect may, nonetheless, be important in areas with strong salinity gradients, which do not show up in smoothed climatological data sets.

Figure 14

In a study of the mixed layer properties in the NwAC at Ocean Weather Station M (OWSM, marked on map in Figure 1), *Nilsen and Falck* [2004] demonstrate a clear correlation between the meridional wind component and the mixed layer salinities during summers. They find the lowest salinities to occur during summers with strong northerly winds, despite the fact that these also are the summers with least precipitation, and suggest that the extra freshwater can only come from the NwCC due to anomalous offshore Ekman transports. Thus, at least during summer, and in regions of relatively strong salinity gradients, it seems that Ekman induced fresh-water transports may be the dominant factor in establishing salinity anomalies. We have no reason to believe that it should be too different during winters, but salinity anomalies will typically be weaker due to deeper mixed layers.

4.3. Mixed Layer Properties

As a first order approximation, the impact on the ocean mixed layer temperature and salinity can be estimated assuming that the ocean is a passive responder to the anomalous forcing. To exemplify, a reduction in heat loss of 10 Wm^{-2} will warm a 100 m thick water column by 0.26°C in four months (December to March), and during the same period of time an increased precipitation of 1 mm day^{-1} will freshen the same water column by 0.04.

If the SSTs are regressed on the NAO-index, the well known tri-pole pattern consisting of colder than normal water from the equator to approximately 20°N, a band of warmer than normal water from Florida towards Europe, and a colder than normal regime in the northwestern North Atlantic emerges [e.g. *Marshall et al.*, 2001b]. For the Nordic Seas region (Figure 15), the response is a general warming along the eastern margins, where the southwesterlies are enhanced during positive NAO years (see Figure 7c), and a cooling in the western part of the region, where the positive NAO years represent stronger northerlies and colder air over the region. Strongest warming is found in the North Sea and Baltic Sea, where the atmospheric forced SST anomalies can exceed 1°C. In contrast, the regions to the west and south of Iceland may become several tenths of degrees colder during positive NAO years. Elsewhere, anomalies are generally small, only of the order of 0.1°C and comparable to the simple estimate given in the introduction to this section.

Figure 15

In contrast to SST, which has been measured regularly by ships for more than a century and by satellites for 25 years, it is not possible to show the direct impact of the anomalous fresh-water fluxes on the SSS by correlating year-to-year changes in SSS with the NAO-index. There are much less data, the NAO response in salinity is weak, and the surface salinity measurements are often noisy due to local precipitation events. Measurements have, nonetheless, shown a general reduction in the surface salinities for the last 3–4 decades [*Blindheim et al.*, 2000; *Furevik et al.*, 2002; *Curry et al.*, 2003], which probably is a combined result of local fresh-water forcing, and a changed balance between the water of Atlantic and Arctic origins.

For the sea-ice extent measurements there are relatively good ship-based data for the last 50 years, and since 1978 space-born passive microwave sensors have covered the Arctic at high temporal and spatial resolutions. A regression of the sea-ice cover on the NAO-index (Figure 16) shows in general, negative values in both the Greenland and Barents Seas, and positive values in the Labrador Sea area. No detrending has been conducted here, and the positive trend in the NAO-index and the negative trends in the sea-ice data in the Nordic Seas are obviously contributing to the negative correlations in the regression values for the Nordic Seas. The sea-ice cover in the Nordic Seas has been decreasing relatively fast during the last decades, and during the record low extent in September 2002 the entire eastern coast of Greenland was ice-free for the first time on record [*Serreze et al.*, 2003]. *Kvingedal* [this volume] has calculated the trend in the Nordic Seas sea-ice extent for the period 1967–2002 and finds a 3.4% per decade decrease in winter sea-ice cover over the 36 year period, which is comparable to the decrease calculated for the entire Arctic since 1978 [*Johannessen et al.*, 1999].

Figure 16

5. OBSERVED CHANGES IN THE NORDIC SEAS OCEAN CLIMATE

It has been known for more than a century that the perhaps single-most important factor for the mild and friendly climate along the northern coasts of Europe is the northern extension of the Gulf Stream. The amount of AW that enters the Nordic Seas has been estimated using indirect methods for decades, and has been directly measured since 1995. Measurements are available from both the Iceland–Faroe and Faroe–Shetland passages, but also from the Svinøy Section extending from the west coast of Norway (marked on map in Figure 1).

There is today surprisingly little consensus about what is actually driving the Atlantic inflow to the Nordic Seas. Three factors seems to be present; the wind forcing, the buoyancy forcing leading to a densification and subsequent sinking of water in the Nordic Seas and the Arctic, and the estuarine forcing which is due to the outflow of PW from the Arctic. For the latter, the mechanism is that the southward flow will entrain ambient water of Atlantic origin, and due to volume conservation there must be a compensating inflow [e.g. *Stigebrandt*, 1981].

Rapid changes in the North Atlantic, Nordic Seas, and Arctic Ocean climate have been indicated from intensified observational programmes, combining new surface, subsurface, and remotely sensed data with historical archives. We will in this section review some of the recent findings, and try to assess how the changes are related to the large-scale changes that have been taking place in the atmospheric circulation over the region. For complementary discussions and references, see also *Visbeck et al.* [2003] and *Blindheim and Østerhus* [this volume].

5.1. Atlantic Inflow

The diverse and variable paths of the source water in the North Atlantic (Figure 1) can be expected to be susceptible to changes in the atmospheric forcing, whether it is variations in the momentum input or variations in the heat- or freshwater fluxes. The main branches of AW feeding the Nordic Seas, the inner branch at the continental slope entering through the FSC, and the outer branch associated with the Arctic Front and entering over the IFR, both seem to be influenced by the large-scale circulation anomalies in the atmosphere.

In a study of surface drifters as well as altimeter data from the period 1992–98, *Flatau et al.* [2003] observed a clear southeastward shift and intensification of the current system in the subpolar North Atlantic during high NAO-index periods. That is, the NAC flow towards the Rockall Trough (Figure 1) is intensified, ultimately giving a stronger flow of AW through the FSC. This seems to be related to findings by *Orvik and Skagseth* [2003b], who compared the volume transport in the eastern branch of the NwAC at the Svinøy Section with the wind stress curl in the North Atlantic. Using 12-month moving averages, the correlation between the Svinøy transport during 7 years and the wind stress curl in a band at 55°N was 0.88, with 15 months time lag. The proposed mechanism for this statistically significant correlation is Ekman pumping altering the density field associated with the NAC at 55°N, forcing a baroclinic Rossby wave, propagating with the baroclinic NAC until it hits the Irish-Scottish

shelf 15 months later, from where fast barotropic waves transport the signal to the Svinøy Section (see Section 4.1).

There are also other indications of a lagged response of the NAO on the ocean circulation within the Nordic Seas, implying that baroclinic adjustment processes take place. *Blindheim et al.* [2000] found that the lateral surface extension of AW in the southeastern Norwegian Sea is negatively correlated with the NAO-index on long (>3 years) time scales, and attributed this to changes in the pathways of the inflow of AW between Iceland and Scotland.

Direct current measurements in the FSC [*Turrell et al.*, 2003] and measurements north of the Faroes capturing the water that flows over the IFR [*Hansen et al.*, 2003] show little interannual variability and a very weak seasonal cycle in the inflow of AW. This is inconsistent with the results by *Flatau et al.* [2003], *Orvik and Skagseth* [2003b], and with the measurements at the Svinøy Section where a seasonal cycle in the eastern branch of the NAC is found [*Orvik et al.*, 2001]. The reason for this apparent discrepancy is not fully understood, but may be related to recirculation of AW and interactions between the two branches in the FSC.

Mork and Blindheim [2000] calculated the geostrophic volume transports in the two branches of the NwAC from hydrographical observations in the Svinøy Section during the years 1955–1996. One of their results was that the two branches appeared to be in opposite phase and NAO controlled since the summer of 1978. This out-of-phase relationship between the outer and inner branches of the NwAC is supported by a model study by *Nilsen et al.* [2003] who found a negative correlation between the flows over the IFR and through the FSC. In their model, the variability in the inflow was linked to an atmospheric pattern resembling the NAO via anomalous Ekman transports and barotropic adjustment processes.

The exact mechanisms linking the anomalous wind field to the inflow is not clear. For the period prior to the mid-seventies, stronger than normal westerlies were associated with a mean wind field that had a component from the North Atlantic Ocean and into the Nordic Seas (Figure 6c), which could support a mechanism with Ekman transport towards the Irish-Scottish shelf, and thus more flow through the FSC. After the mid-seventies, the pattern is much more zonal, and it is difficult to see how the inflow can be forced by the local wind. However, dynamical consideration (flow tends to follow f/H contours) and model results [*Nilsen et al.*, 2003] suggest that there is a tight link between the inflow in the FSC and the outflow through the Denmark Strait. The northerly winds along the eastern coast of Greenland, together with the increased southward extension of PW thus associated with high NAO-index may inhibit inflow of AW both in the Denmark Strait [*Blindheim et al.*, 2000] and over the IFR [*Hansen and Kristiansen*, 1994], enhancing the eastward shift of the Atlantic inflow and NAO control of the flux along the eastern slope (North Atlantic/Norwegian Sea). The NAO related variability in the inflow might thus just as well be forced by the northerly winds along the coast of Greenland, and an associated enhanced flow through the Denmark Strait, as it is forced locally at or near the inflowing region. Comparing the two periods, before and after the mid-seventies, it follows that the explanation involving enhanced outflow and a compensating inflow seems to be the most plausible for the latter period (Figure 6d). This is also the period showing highest correlation between the NAO and Fram Strait ice export [*Hilmer and Jung*, 2000], as will be further discussed in the next section.

5.2. Fram Strait Freshwater and Ice Export

The main export route of Arctic sea-ice and freshwater goes through the Fram Strait, where an estimated amount of 2000–3000 km^3 of sea-ice and 1000 km^3 of liquid freshwater escape the Arctic every year [see *Aagaard and Carmack*, 1989; *Vinje et al.*, 1998; *Kwok et al.*, 2004]. Variability in the strength of the export is of importance not only for the freshwater budget of the Arctic, but also for the downstream ocean properties and deep-water formation in the Greenland, Irminger, and Labrador Seas.

The freshwater export is a difficult parameter to measure, and most estimates are based on coupled Arctic ocean-sea ice models. Forcing their model with the NCEP/NCAR reanalysis data, *Zhang et al.* [2003] found that the leading atmospheric mode was the driver of many of the changes observed in the

Arctic. When their Arctic Oscillation index changed from a negative to a positive phase, the freshwater and sea-ice export through the Fram Strait increased by 12% and 56%, respectively.

The single most important factor for the ice export through the Fram Strait is, to the best of our knowledge, the SLP gradient across the strait. Using almost 3 years of data from a moored Doppler current meter in the Fram Strait, *Widell et al.* [2003] found the correlation between measured ice velocities and the SLP gradient (calculated from NCEP/NCAR reanalysis data) to be as high as 0.76 for daily means and 0.79 for monthly means.

By tracking common features in successive satellite images of sea-ice, *Kwok et al.* [2004] managed to estimate the sea-ice area flux through the Fram Strait for the period 1978–2002 and found a correlation of 0.62 with the wintertime NAO-index. This seems to contradict the fact that the very large outflow of sea-ice and freshwater during the late '60s, responsible for the great salinity anomalies observed in the subpolar gyre and later along the AW pathways in the Nordic Seas [*Dickson et al.*, 1988], occurred during a period characterized by a very weak Icelandic low. However, using composites for the low-index years 1963–1969, *Dickson et al.* [2000] showed that the pressure pattern gave a northerly wind component over the Fram Strait also in those years, despite the weak NAO.

Based on a hindcast run with an ocean-sea-ice model, *Hilmer and Jung* [2000] demonstrated that the correlation between the NAO and Fram Strait sea-ice export breaks down when the time series are extended back in time. While they found a similar correlation as *Kwok et al.* [2004] when using the same period, the correlation dropped to almost zero for the period 1958–1977. And extending their analysis to a century-scale control integration of a coupled climate model, they demonstrated that the correlation found in the last two decades was unusually high [*Jung and Hilmer*, 2001].

In a recent study, *Schmith and Hansen* [2003] used historical observations of multiyear ice from the southwest Greenland for the period 1820–2001 as a proxy to deduce the Fram Strait ice export. From their reconstructions, they find relatively large interdecadal variability, with high ice export values around 1900 and in the '60s, and lowest values in the 1820s and in the 1930s and '40s. As high ice export values correspond to cold SST periods in the North Atlantic and vice versa, they suggest that the temperature anomalies in the North Atlantic may be a response to the ice export. They further used their observational data to redo the calculations of *Jung and Hilmer* [2001] using model data and demonstrated the shifting influence of the NAO on the Fram Strait ice export.

The changing influence of the NAO, or more precisely, the changing representativeness of the traditional NAO-index when it comes to describing the sea-level gradient across the Fram Strait, can be seen in Figure 6c,d. During the first half of the reanalysis period, when the NAO-index was relatively low, high-index values represent a low centered west of Iceland, with a modest SLP gradient over the Fram Strait (Figure 6c). For the period prior to the '70s, the NAO-index is therefore not representing the wind conditions in the Fram Strait. It is instead, as Figure 6c suggests, a better proxy for the northerly winds over the Canadian Archipelago and the Davis Strait, where *Hilmer and Jung* [2000] found the correlation between ice export and the NAO-index to be 0.63 for the early period (until 1978). For the latter period, the SLP pattern has changed (Figure 6d). Now the NAO is in a more positive phase, and the index is better representing the SLP gradient across the Fram Strait. High-index values are now corresponding to northerlies in the Fram Strait, driving more ice out of the Arctic. For the Davis Strait ice export, the NAO is not a good proxy for this latter period, as *Hilmer and Jung* [2000] calculated the correlation to be only 0.13 for the period after 1978.

5.3. Nordic Seas Circulation

As for the inflow of the AW to the Nordic Seas, it is not clear what is driving the circulation within the seas; whether it is driven by the inertia of the inflow, local winds, or buoyancy forcing within the basins. An early attempt to study the effect of the positive wind stress curl in the area (e.g. Figure 7) was made by *Aagaard* [1970] who digitalized hand drawn six-hourly weather maps for 1965 and calculated the monthly mean Sverdrup transports for the Nordic Seas. The annual-mean wind-driven gyre transport exceeded 30 Sv in his calculations, which was comparable to the 35 Sv *Aagaard and Coachman* [1968] estimated from measurements at the western side of the gyre. The variations

from month to month were tremendous, ranging from practically zero to almost 90 Sv.

In a recent study, *Nøst and Isachsen* [2003] combined the divergence in the Ekman transports and the observed climatological density field to calculate the geostrophic flow along f/H contours within the Nordic Seas–Arctic Ocean and got circulation patterns in close agreement with the existing observations [*Poulain et al.*, 1996; *Orvik and Niiler*, 2002; *Jakobsen et al.*, 2003]. Generally, the bottom flow and the surface flow were aligned. A noticeable exception was in the Lofoten Basin, where the model gave cyclonic bottom flow and anti-cyclonic surface flow, the latter in agreement with drifter measurements [*Jakobsen et al.*, 2003]. Using the assumption of a constant transport in the western branch of the NwAC, *Orvik* [2004] found the reverse deep flow to be the cause for the large deepening of the Atlantic layer in the Lofoten Basin area.

Skagseth et al. [2004] have used the combined Topex-Poseidon and ERS 1/2 weekly-mean sea-level anomaly (SLA) data [*Ducet et al.*, 2000] and current meter measurements to look at coherent signals along the continental slope from the Irish-Scottish shelf towards the Fram Strait. They first compared the weekly-mean geostrophic velocity derived from the SLA data with direct measurements at the Svinøy Section, and found an overall correlation of 0.55 over a 7 year period. The discrepancy was mainly due to high-frequency mesoscale variability in the direct measurements that was not resolved in the altimeter data. They further found the flow along the slope to be forced by anomalies in SLP resembling the NAO pattern, with no phase lag.

Using the same dataset as *Skagseth et al.* [2004], we have calculated the phase of the annual cycle of the SLA (Figure 17a). A strong topographic control on the SLA can be seen from the depth dependency of the time of annual maximum. For instance, note that the shallow areas around Iceland and on the continental shelf from Ireland to the Barents Sea and Fram Strait have SLA maximum later in the year than the central parts of the Nordic Seas and the North Atlantic. This feature can not be fully explained by the annual cycle in heat fluxes (not shown), but must be interpreted as the combination of pile up of water due to anomalous Ekman transports, and the strong f/H control of the flow. The same conclusion can be drawn from an extension of the work by *Nøst and Isachsen* [2003], who find that the main difference between summer and winter circulation is a strengthening of the flow along the f/H contours during winters (Nøst, personal communication, 2004).

Figure 17

In Figure 17b the correlation between the Lisbon-Iceland NAO index [*Hurrell*, 1995] and the SLA data is shown. While the seasonal cycle in both data sets has been removed, nothing has been done to eliminate the steric effect on the SLAs, which will contribute to the high elevations in the North Sea, along the Norwegian coast, and in the Barents Sea due to less heat loss and more precipitation (Figures 9d and 10d). Highest correlations between the SLA and the NAO-index (Figure 17b) are found west of Denmark and in the Baltics, where correlations exceed 0.4, and a unit increase in NAO-index corresponds to a 5 cm increase in sea level (not shown). The correlation pattern is consistent with an increased cyclonic wind stress curl over the Nordic Seas, where divergence in the Ekman transports makes a negative SLA in the central basin, and positive SLA along the surrounding coast lines. Thus, associated with stronger than normal westerlies, the northward flow of AW should be stronger than normal. This fits with measurements from the Svinøy Section where *Orvik et al.* [2001] revealed a strong correlation between the NAO-index and the eastern branch of the NwAC, even on intra-seasonal time scales.

While surface drifters, altimeter data, and direct current meter measurements have revealed substantial information about the upper ocean circulation, much less is known about the intermediate and abyssal circulation of the Nordic Seas. Much of the knowledge we have about transport rates and transport times of the intermediate Nordic Seas, originate from the SF_6 release experiment in the central Greenland Sea in 1996 [*Watson et al.*, 1999]. Using an advective-diffusive model applied on output from a numerical model experiment, *Eldevik et al.* [this volume] manage to capture the main features of the observations. According to their model, the SF_6 enriched water reached the Faroe Bank overflow 2 years after the release, and the Denmark Strait one year later, in good agreement with observations. The authors further point to the huge differences in the intermediate circulation patterns during the different periods in the 50 years model run, and believe the differences are caused

by variations in the large-scale atmospheric forcing. During the SF_6 period after September 1996, the tracer went straight to the FSC following the Jan Mayen Current. In contrast, for other periods the tracer could have taken a longer route with the East Greenland and East Icelandic Currents before reaching the Faroe Bank overflow, and have used more than twice the time it needed during the SF_6 experiment.

While there are indications of variations in the pathways leading to the overflow sites, there are also reports of changes in the strength of the overflow. Using OWSM data, *Hansen et al.* [2001] showed a 50 years decrease in the height of the $\sigma_\theta = 28$ density level, and by analytical arguments and comparison with direct measurements of the Faroe Bank overflow, deduced a 20% reduction in the overflow during the same period. Measurements by direct methods do not show a reduction in the inflow of AW, but these records are of shorter duration than the above-mentioned studies. For instance, seven years of direct measurements in the eastern branch of the inflowing AW at the Svinøy Section show no indications of a reduction of the transport of AW into the area [*Orvik et al.*, 2001; *Orvik and Skagseth*, 2003a]. Combined with the above, this should imply that a reduction of the overflow could be associated with a reduced transport in the western branch that crosses the IFR. It also fits with the expected responses to the increased westerlies, that more water should move east towards the slope current off the Irish-Scottish shelf.

The results of model simulations are not conclusive, and the relatively weak changes in the thermohaline structures and deep circulation may often be difficult to distinguish from model drifts and other sources of errors. There nonetheless exist hindcast simulations with an isopycnic ocean model integrated from 1948 showing a reduction in the inflow of AW that quantitatively agrees with the estimates made by *Hansen et al.* [2001], and which points to the reduced inflow over the IFR as the cause [*Nilsen et al.*, 2003].

5.4. Nordic Seas Hydrography

Due to traditions going back to the pioneering works in the late 19th century [see *Blindheim and Østerhus*, this volume, for references], the Nordic Seas are among the most well sampled regions in the world. During the last few decades, several pronounced and far-reaching changes in the hydrography have been related to the low-frequency variability in the atmospheric circulation, with the record weak westerlies in the 1960s and the record strong westerlies in the '90s, as the two extremes. We will here limit the discussion to the observed warming of the AW, the freshening of the intermediate water, and the warming of the deep water.

Furevik [2000, 2001] used both satellite derived SST data and direct measurements to study the transport of heat anomalies from the FSC towards the Barents Sea and Arctic Ocean during the '80s and '90s (Figure 18). Two warm (W1 and W2) and one cold (C1) period were discussed. *Furevik* [2001] concluded that while the warm and cold anomalies of the '80s were advected with the AW from the FSC and through the Nordic Seas, the stronger anomaly during the early part of the '90s was a response to reduced heat loss in the Nordic Seas. His arguments were based on the observations that firstly, this heat anomaly is barely seen in the inflowing region, but increases in strength towards north (Figure 18a), and secondly, in the Barents Sea Opening the heat anomaly starts in the surface and gradually penetrates deeper (Figure 18b). Model studies by *Karcher et al.* [2003] mainly support this interpretation, but also point to an increased inflow of AW to the Nordic Seas as a cause for the warm anomaly of the '90s.

Figure 18

A third factor may also be weaker transport in the western branch and stronger transport in the eastern branch of the NwAC, as indicated by an eastward [*Blindheim et al.*, 2000] and southward [*Furevik et al.*, 2002] displacement of the S=35 isohaline in the southern Norwegian Sea. Thus, simple theory involving topographical steering implies that less AW should be recirculated in the Nordic Seas, and furthermore suggests that an eastward displacement of the AW should force a relatively larger portion of the water through the Barents Sea. This has been shown in model runs using both idealistic [*Furevik*, 1998] and real [*Zhang et al.*, 1998] topography. Further to the north, the anomalous warm water that entered through the Fram Strait and the Barents Sea in the early '90s, and a shift to a

more cyclonic atmospheric circulation over the Arctic, were apparently responsible for a significant warming and expansion of the AW layer in the Arctic Ocean [*Carmack et al.*, 1995, 1997; *Swift et al.*, 1997; *Morison et al.*, 1998; *Grotefendt et al.*, 1998; *Karcher et al.*, 2003].

Below the surface layers, the Nordic Seas have experienced a widespread freshening since the '60s with record weak westerlies, to the '90s when the westerlies have been the strongest measured [*Blindheim et al.*, 2000; *Dickson et al.*, 2002]. Averaged over the depth interval 400–1500 m at the OWSM, the magnitude of this freshening is 0.023, corresponding to mixing 0.7 m of freshwater to the water column. The depth of the freshening reaches far below the sill depths of the overflow water to the North Atlantic, and the freshening signal is therefore being exported to the North Atlantic. From the 1960s to year 2000 the salinity of the overflow water typically decreased by 0.01/decade [*Turrell et al.*, 1999; *Dickson et al.*, 2002]. Over a 40-year interval this corresponds to adding 1.2 m of freshwater to a 1000 m thick water column. While sinking, the overflow water mixes with ambient water that is itself freshening, thus preserving or even amplifying the freshening signal downstream into the Labrador Sea and eventually into the deep western boundary current towards the south.

It is not clear where the excess freshwater is coming from, but several factors have been proposed, including more ice and freshwater export from the Arctic [*Vinje*, 2001; *Zhang et al.*, 2003; *Kwok et al.*, 2004], more precipitation over the region (see Figure 10d), and internal redistribution of water masses [*Blindheim et al.*, 2000] where AW is replaced by PW in the central Nordic Seas. In a recent study, *Curry et al.* [2003] used the Levitus data [e.g. *Levitus et al.*, 2000] for the Atlantic Ocean to study the changes in ocean salinity from the '60s to the '90s in a transect from 50°S to 60°N. The result of this study was a deep-reaching freshening in both the southern and northern high latitudes, and more saline water occupying the upper 100m at low latitudes. This is a strong indication of an enhanced hydrological cycle, with more evaporation in the low latitudes and more precipitation in the high latitudes, which in most climate models are the predicted responses to global warming [e.g. *Cubasch et al.*, 2001].

Since the '60s, when the temperatures in the deep water of the Nordic Seas reached a minimum, the deep-water formation in the Greenland Sea has been strongly reduced or absent [*Dickson et al.*, 1996], and the Greenland Sea Bottom Water has gradually warmed [*Budéus et al.*, 1998], at least partly due to inflow of warmer water from the Eurasian Basin [*Meincke et al.*, 1997]. With a few years time lag the warming was observed at 2000m depth at OWSM, where the signal gradually rose in the water column [*Østerhus and Gammelsrød*, 1999]. The two authors also demonstrated a reversal of the deep flow between the Greenland Sea and the Norwegian Sea, and suggested this was a consequence of a reversal of the density gradient between the two basins.

6. DISCUSSION - NORDIC SEAS AND CLIMATE CHANGE

Observations have shown that during the last decades the atmospheric westerlies have strengthened, the deep-water formation in the Greenland Sea has weakened, the sea-ice extent and thickness have been strongly reduced, and the deep water of the North Atlantic has become fresher. And we may ask: Are we witnessing the impacts of global change, or are the recent observations just low-frequency manifestations of stochastic noise in the complex and still little understood atmosphere-ice-ocean climate system?

6.1. Changes in the Surface Ocean

During the period with NCEP/NCAR reanalysis data, the strength of the westerlies has undergone a change from record weak conditions in the '60s to record strong conditions in the '90s. The changes in heat fluxes and ocean surface properties over the same time interval can be assessed by comparing the two 15-year periods 1958–1972 and 1988–2002 (Figure 19). The pictures that emerge are close to what is found by simply multiplying the changes in the NAO-index with the regression patterns shown in the previous sections. In general, this includes a more cyclonic winter air flow over the Nordic Seas region (compare with Figure 5b), increased wind stress (Figure 8b), reduced heat loss to the atmosphere (Figure 9d), and increased precipitation (Figure 10d). Along the east coast of Greenland,

Figure 19

increased northerly winds and less sea-ice have resulted in increased heat and freshwater fluxes to the atmosphere. At the ocean surface the same period reveals a significant decrease in SST to the southwest, and a warming mainly confined to the Barents Sea, the North Sea, and the Baltic Sea to the east. Furthermore, there is a substantial retreat of the sea-ice edge both in the Greenland and Barents Sea areas.

While most of the changes in the surface conditions can be explained as local responses to the variations in the atmospheric forcing, the SST and sea-ice concentration fields also indicate that changes in the ocean circulation play an active role. Two noticeable areas are to the east and west of Iceland, where there has been significant cooling despite reduced heat loss to the atmosphere. Here the AW seems to be replaced by water of polar origin, probably a result of decreased inflow of AW in the Irminger and IFR branches, and perhaps also increased outflow from the Arctic. This view is also supported by many observations and model results cited in Sections 5.1 and 5.2. A contributing factor east of Iceland may also be anomalous Ekman transports (e.g. Figure 13) associated with the strengthened atmospheric circulation (Figure 19b). The SST plot (Figure 19e) further show the strong warming in the northern extensions of the NwAC, both in the branch flowing through the Barents Sea and the branch going into the Fram Strait, that eventually is tied to the recent warming of the Arctic.

6.2. Changes in the Deep Ocean

Being one of the main formation areas for the deep water that ventilates the world oceans, the Nordic Seas and the water mass conversion taking place there may play a pivotal role for the climate far outside its boundaries. One of the many issues that have been discussed is the role of the deep-water formation in the Nordic Seas when it comes to the strength of the NAC and the inflow of AW to the Nordic Seas, and the general heat transport towards northern Europe.

Early experiments with simplified climate models indicated that we may expect a total shutdown of the AMOC in a future climate with CO_2 induced global warming [*Rahmstorf and Ganopolski*, 1999], while most state-of-art fully 3-dimensional climate models today indicate a more modest but still significant reduction [*Cubasch et al.*, 2001]. The main reason is a strengthened hydrological cycle, giving increased precipitation to the high latitudes, which in addition to general warmer surface water reduces the density and stabilizes the water columns in the sinking regions. In most models the reduction in the strength of the AMOC starts towards the end of the previous century.

Since the '60s, the Nordic Seas have undergone changes in hydrography that are unprecedented in instrumental records. From a regime with strong and deep reaching Greenland Sea convection during wintertime, producing a very cold and dense bottom water, the convection is now shallow and occurring irregularly. The result has been a warming and a lowering of the densities of the Nordic Seas, a decrease in the density difference across the GSR, and a possible 20% reduction in the Faroe Bank overflow. In addition, there has been a pronounced freshening of the intermediate depths of the Nordic Seas. This is seen as a long-term freshening trend in the overflow water and has resulted in a freshening of most of the deep North Atlantic. It may thus seem that the observational evidence supports the climate models when they predict a reduction in the AMOC during global warming, and that such a reduction is already taking place.

There are, however, recent results that question this conclusion. Using the Hadley Centre's coupled climate model, *Wu et al.* [2004] found a freshening in their ensemble run that resembled the observed freshening of the North Atlantic and Nordic Seas, without this being accompanied by a weaker AMOC. The simulated AMOC was in fact strengthened during the same period. Furthermore, the newest measurements from the Faroe Bank overflow show an increased export of dense overflow water during the last two years (Bogi Hansen, personal communication, 2004), questioning the significance of the previously reported downward trend.

6.3. Nordic Seas in a Future Climate

With all the changes that have been observed in the Nordic Seas climate during the recent decades, and the growing evidence that the changes may be linked to the greenhouse gas forcing through a

strengthening of the westerlies, it is tempting to speculate about the future state of the Nordic Seas.

Based on the literature reviewed in this paper, our first and strongest working hypothesis is that most of the changes we have seen in the Nordic Seas's circulation and hydrography since the '60s and onward, are an inevitable response to the deepening of the Icelandic low and the associated strengthening of the westerlies [e.g. *Marshall et al.*, 2001b; *Visbeck et al.*, 2003]. Our second hypothesis is that the decadal to multidecadal variability in the atmospheric circulation is linked to the increased concentration of CO_2 and other greenhouse gases, either due to **warmer tropical waters** [e.g. *Hoerling et al.*, 2001], or due to increased north-south temperature contrasts as a response to a warmer troposphere and a colder stratosphere [e.g. *Shindell et al.*, 1999]. Our third hypothesis is that the northeastward extension of the storm tracks, and thus the eastward displacement of the northern centre of action, is linked to the strengthening of the westerlies [e.g. *Cassou et al.*, 2004]. And our forth hypothesis is that the temporal and spatial trends seen in the NAO in the second half of the 20th century will be sustained or even amplified during the years ahead [e.g. *Fyfe et al.*, 1999; *Ulbrich and Christoph*, 1999].

In order to assess what the consequences will be for the Nordic Seas climate, we may either rely on integrations with coarse climate models and successive dynamical downscaling with finer models, or on what we already know about the processes that are important for the present day Nordic Seas climate, and discuss how these processes may be affected by climate change. We will here take the latter approach.

The Nordic Seas ocean climate will be determined by the local atmosphere-ocean fluxes, and the volume and properties of the warm, saline water entering from the south, and the cold, fresh water entering from the north. If the long-term trend in the NAO is sustained, a reduced heat loss to the atmosphere and increased precipitation and river runoff will work to stabilize the water column, and thus reduce the convection depths within the Nordic Seas. Together with the observations of the relatively strong stratification of the present day Greenland Sea compared to the '60s, it is unlikely that the open-ocean deep-water formation will recover. An exception is for a scenario with many successive cold winters or with more saline water being advected into the region. Thus, we may anticipate a continuation of the warming of the deep water, the freshening of the intermediate water, and perhaps an even further reduction in the rate of overflow.

Changes in the atmospheric forcing will most likely impact all mechanisms that are keeping the relatively stable inflow of warm AW to the Nordic Seas, and competitive effects may occur. Firstly, a reduced ice cover will mean more water is exposed to winter cooling, which can lead to a higher production of deep water both by brine release on the shelves, and due to open ocean convections in new ice-free areas [e.g. *Aagaard and Carmack*, 1989]. Secondly, a strengthened hydrological cycle [*Curry et al.*, 2003] in combination with thinner ice [e.g. *Rothrock et al.*, 2003] will increase the liquid freshwater export through the Fram Strait. This can have large consequences for the inflow, as more freshwater will, by mixing with the water below, strengthen the estuarine circulation and thus also strengthen the compensating inflow of AW [see *Stigebrandt*, 1981]. And thirdly, with a stronger wind stress curl over the North Atlantic, we may expect a stronger inflow of AW to the Nordic Seas. Based on model results and observational data, the increase will likely occur through the FSC, while there may actually be a reduced inflow over the IFR [e.g. *Mork and Blindheim*, 2000; *Nilsen et al.*, 2003].

On long time scales, the local buoyancy effects of the strengthened atmospheric circulation may be reduced or perhaps canceled if the northward flow of AW carries colder and more saline water to the north. Two factors that may contribute to this are the observed enhanced cooling over the north Atlantic during positive NAO years [e.g. *Delworth and Dixon*, 2000; *Marshall et al.*, 2001b], and the increased evaporation over the tropical regions due to a spin-up of the hydrological cycle [e.g. *Curry et al.*, 2003].

To conclude, we find it likely that recent trends in the Nordic Seas climate are strongly tied to global climate change, and that these changes will persist or even amplify in the decades ahead of us. We further believe that the inflow of AW to the Nordic Seas is a robust feature driven by the combined effect of deep-water formation north of the GSR, the estuarine circulation effects, and the forcing from the wind. The effect of global warming is likely to favor some and disfavor other mechanisms, and in

total we find it unlikely that we are facing a total shutdown of the AMOC or other dramatic changes in the ocean circulation in the near future.

7. SUMMARY AND CONCLUDING REMARKS

In this paper the large-scale atmospheric circulation impacts on the Nordic Seas ocean climate have been reviewed. The Icelandic low and the Azores high, giving prevailing southwesterly winds to the southeastern part of the Nordic Seas, and easterly and northeasterly winds in the northwestern part of the region, dominate the climate in the North Atlantic region. During the last decades the large-scale atmospheric circulation has undergone a low-frequency shift from record weak westerlies in the '60s to record strong westerlies in the '90s. Associated with this shift, the changes in the atmospheric momentum, heat, and freshwater forcing seem to be responsible for many of the astonishingly large changes observed in the Nordic Seas' circulation and hydrography over the same period. Both local and remote processes seem to play an active role in the atmospheric forcing of the ocean.

The strengthening of the westerlies is concurrent in time with the strong increase in global mean temperatures since the '60s, which is likely linked to the increased concentrations of atmospheric greenhouse gases. The connection between global warming and strengthened westerlies is still debated. Recent dynamical considerations, however, and model experiments have pointed to tropical SSTs and in particular SSTs in the Indian Ocean as a likely source for the energy causing the spin-up of the system. If this is the case, and if the increasing concentration of atmospheric CO_2 continues to increase the tropical temperatures, we may expect that the recent trend towards stronger westerlies will be sustained. If so, the most extreme conditions observed in the ocean climate of the North Atlantic, Nordic Seas, and the Arctic during the last decades may be only previews of the years lying ahead of us.

Acknowledgments. The study has been supported by the Research Council of Norway through the NoClim (TF) and RegClim (JEØN) projects, and by the G. C. Rieber Foundations (JEØN). The work was completed during a visit of TF at the Danish Meteorological Institute in Copenhagen whom he will thank for hospitality and good working environment. The authors will also thank John Walsh and two anonymous reviewers for their constructive comments to the manuscript. The NCEP/NCAR Reanalysis data are provided by the NOAA-CIRES Climate Diagnostics Center, Boulder, Colorado, USA, from their Web site at http://www.cdc.noaa.gov/. This is contribution no. 68 from the Bjerknes Centre for Climate Research.

REFERENCES

Aagaard, K., Wind-driven transports in the Greenland and Norwegian seas, *Deep-Sea Res.*, *17*(2), 281–291, doi:10.1016/0011-7471(70)90021-5, 1970.

Aagaard, K., and E. Carmack, The role of sea ice and other fresh water in the arctic circulation, *J. Geophys. Res.*, *94*(C10), 14,485–14,498, 1989.

Aagaard, K., and L. K. Coachman, East Greenland Current north of Denmark Strait: Part I, *Arctic*, *21*(3), 181–200, 1968.

Alexander, M. A., U. S. Bhatt, J. E. Walsh, M. S. Timlin, J. S. Miller, and J. D. Scott, The atmospheric response to realistic Arctic sea ice anomalies in an AGCM during winter, *J. Climate*, *17*(5), 890–905, doi: 10.1175/1520-0442(2004)017, 2004.

Ambaum, M. H. P., and B. J. Hoskins, The NAO troposphere-stratosphere connection, *J. Climate*, *15*(14), 1969–1978, 2002.

Ambaum, M. H. P., B. J. Hoskins, and D. B. Stephenson, Arctic Oscillation or North Atlantic Oscillation?, *J. Climate*, *14*(16), 3495–3507, 2001.

Anderson, D. L. T., and A. E. Gill, Spin-up of a stratified ocean, with application to upwelling, *Deep-Sea Res.*, *22*(9), 583–596, 1975.

Anderson, D. L. T., and P. D. Killworth, Spin-up of a stratified ocean, with topography, *Deep-Sea Res.*, *24*(8), 709–732, 1977.

Baldwin, M. P., and T. J. Dunkerton, Downward propagation of the Arctic Oscillation from the stratosphere to the troposphere, *J. Geophys. Res.*, *104*(D24), 30,937–30,946, doi:10.1029/1999JD900445, 1999.

Baldwin, M. P., D. B. Stephenson, D. W. J. Thompson, T. J. Dunkerton, A. J. Charlton, and A. O'Neill, Stratospheric memory and extended-range weather forecasts, *Science*, *301*(5633), 636–640, doi: 10.1126/science.1087143, 2003.

Bengtson, L., V. A. Semenov, and O. M. Johannessen, The early century warming in the Arctic - a possible mechanism, *J. Climate*, in press, 2004.

Bengtsson, L., E. Roeckner, and M. Stendel, Why is the global warming proceeding much slower than expected?, *J. Geophys. Res.*, *104*(D4), 3865–3876, doi:10.1029/1998JD200046, 1999.

Bjerknes, J., Synoptic survey of the interaction of sea and atmosphere in the North Atlantic, *Geophys. Norv.*, *24*(3), 115–145, 1962.

Bjerknes, J., Atlantic air–sea interaction, *Adv. Geophys.*, *10*, 1–82, 1964.

Blindheim, J., V. Borovkov, B. Hansen, S. A. Malmberg, W. R. Turrell, and S. Østerhus, Upper layer cooling and freshening in the Norwegian Seas in relation to atmospheric forcing, *Deep-Sea Res. I*, *47*(4), 655–680, doi:10.1016/S0967-0637(99)00070-9, 2000.

Bower, A. S., P. L. Richardson, H. D. Hunt, T. Rossby, M. D. Prater, H.-M. Zhang, S. Anderson-Fontana, P. Perez-Brunius, and P. Lazarevich, Warm-water pathways in the Subpolar North Atlantic: An overview of the ACCE RAFOS float programme, *Int. WOCE Newsl.*, *38*, 14–16, 2000.

Budéus, G., W. Schneider, and G. Krause, Winter convective events and bottom water warming in the Greenland Sea, *J. Geophys. Res.*, *103*(C9), 18,513–18,527, doi:10.1029/98JC01563, 1998.

Carmack, E. C., R. W. Macdonald, R. G. Perkin, F. A. McLaughlin, and R. J. Pearson, Evidence for warming of Atlantic Water in the southern Canadian Basin of the Arctic Ocean: Results from the Larsen-93 expedition, *Geophys. Res. Lett.*, *22*(9), 1061–1064, doi:10.1029/95GL00808, 1995.

Carmack, E. C., et al., Changes in temperature and tracer distributions within the Arctic Ocean: Results from the 1994 Arctic Ocean section, *Deep-Sea Res. II*, *44*(8), 1487–1493, doi:10.1016/S0967-0645(97)00056-8, 1997.

Carr, M., and H. Rossby, Pathways of the North Atlantic Current from surface drifters and subsurface floats, *J. Geophys. Res.*, *106*(C3), 4405–4419, doi:10.1029/2000JC900106, 2001.

Cassou, C., L. Terray, J. W. Hurrell, and C. Deser, North atlantic winter climate regimes: Spatial asymmetry, stationarity with time, and oceanic forcing, *J. Climate*, *17*(5), 1055–1068, doi:10.1175/1520-0442(2004)017, 2004.

Cubasch, U., G. Meehl, G. Boer, R. Stoffer, M. Dix, A. Noda, C. Senior, S. Raper, and K. Yap, *Projections of Future Climate Change*, chap. 9, pp. 525–582, Cambridge University Press, Cambridge, United Kingdom and New York, NY, USA, 2001.

Curry, R., R. R. Dickson, and I. Yashayaev, A change in the freshwater balance of the Atlantic Ocean over the past four decades, *Nature*, *426*(6968), 826–829, doi:10.1038/nature02206, 2003.

Czaja, A., A. W. Robertson, and T. Huck, The role of Atlantic ocean–atmosphere coupling in affecting North Atlantic Oscillation variability, in *The North Atlantic Oscillation: Climatic Significance and Environmental Impact*, *Geophysical Monograph Series*, vol. 134, edited by J. W. Hurrell, Y. Kushnir, G. Ottersen, and M. Visbeck, pp. 147–172, AGU, doi:10.1029/134GM07, 2003.

Delworth, T. L., and K. W. Dixon, Implications of the recent trend in the Arctic/North Atlantic Oscillation for the North Atlantic thermohaline circulation, *J. Climate*, *13*(21), 3721–3727, doi:10.1175/1520-0442(2000)013<3721:IOTRTI>2.0.CO;2, 2000.

Deser, C., On the teleconnectivety of the "Arctic Oscillation", *Geophys. Res. Lett.*, *27*(6), 779–782, doi:10.1029/1999GL010945, 2000.

Dickson, B., I. Yashayaev, J. Meincke, B. Turrell, S. Dye, and J. Holfort, Rapid freshening of the deep North Atlantic Ocean over the past four decades, *Nature*, *416*(6883), 832–837, doi:10.1038/416832a, 2002.

Dickson, R., J. Lazier, J. Meincke, P. Rhines, and J. Swift, Long-term coordinated changes in the convective activity of the North Atlantic, *Prog. Oceanogr.*, *38*(3), 241–295, doi:10.1016/S0079-6611(97)00002-5, 1996.

Dickson, R., T. Osborn, J. Turrell, J. Meincke, J. Blindheim, B. Ådlandsvik, T. Vinje, G. Alekseev, and W. Maslowski, The Arctic Ocean response to the North Atlantic Oscillation, *J. Climate*, *13*(15), 2671–2696, doi:10.1175/1520-0442(2000)013<2671:TAORTT>2.0.CO;2, 2000.

Dickson, R. R., J. Meincke, S.-A. Malmberg, and A. J. Lee, The "Great Salinity Anomaly" in the northern North Atlantic 1968–1982, *Prog. Oceanogr.*, *20*(2), 103–151, doi:10.1016/0079-6611(88)90049-3, 1988.

Ducet, N., P. Y. LeTraon, and G. Reverdin, Global high-resolution mapping of ocean circulation from Topex/Poseidon and ERS-1 and -2, *J. Geophys. Res.*, *105*(C8), 19,477–19,498, doi:10.1029/2000JC900063, 2000.

Flatau, M. K., L. Talley, and P. P. Niiler, The North Atlantic Oscillation, surface current velocities, and SST changes in the Subpolar North Atlantic, *J. Climate*, *16*(14), 2355–2369, doi:10.1175/2787.1, 2003.

Furevik, T., On the Atlantic Water flow in the Nordic Seas: Bifurcation and variability, Dr. scient. thesis in physical oceanography, Geophysical Institute, Univ. Bergen, Allégt. 70, 5007 Bergen, Norway, 1998.

Furevik, T., On anomalous sea surface temperatures in the Nordic Seas, *J. Climate*, *13*(5), 1044–1053, doi:10.1175/1520-0442(2000)013<1044:OASSTI>2.0.CO;2, 2000.

Furevik, T., Annual and interannual variability of Atlantic Water temperatures in the Norwegian and Barents Seas: 1980–1996, *Deep-Sea Res. I*, *48*(2), 383–404, doi:10.1016/S0967-0637(00)00050-9, 2001.

Furevik, T., M. Bentsen, H. Drange, J. A. Johannessen, and A. Korablev, Temporal and spatial variability of the sea surface salinity in the Nordic Seas, *J. Geophys. Res.*, *107*(C12), 8009, doi:10.1029/2001JC001118,

2002.
Furevik, T., M. Bentsen, H. Drange, I. Kindem, N. Kvamstø, and A. Sorteberg, Description and evaluation of the Bergen Climate Model: ARPEGE coupled with MICOM, *Clim. Dynam.*, *21*(1), 27–51, doi:10.1007/s00382-003-0317-5, 2003.
Fyfe, J. C., G. J. Boer, and G. M. Flato, The Arctic and Antarctic Oscillations and their projected changes under global warming, *Geophys. Res. Lett.*, *26*(11), 1601–1604, doi:10.1029/1999GL900317, 1999.
Gascard, J.-C., C. Kergomard, P.-F. Jeannin, and M. Fily, Diagnostic study off the Fram Strait Marginal Ice Zone during summer from 1983 and 1984 Marginal Ice Zone Experiment. Lagrangian observations, *J. Geophys. Res.*, *93*(C4), 3613–3641, doi:10.1029/88JC01488, 1988.
Gill, A. E., *Atmosphere-Ocean Dynamics*, 662 pp., Academic Press, London, 1982.
Gillett, N. P., H. Graf, and T. J. Osborn, Climate change and the North Atlantic Oscillation, in *The North Atlantic Oscillation: Climatic Significance and Environmental Impact*, *Geophysical Monograph Series*, vol. 134, edited by J. W. Hurrell, Y. Kushnir, G. Ottersen, and M. Visbeck, pp. 173–192, AGU, doi:10.1029/134GM09, 2003.
Grotefendt, K., K. Logemann, D. Quadfasel, and S. Ronski, Is the Arctic Ocean warming?, *J. Geophys. Res.*, *103*(C12), 27,679–27,687, doi:10.1029/98JC02097, 1998.
Hansen, B., and R. Kristiansen, Long-term changes in the Atlantic water flowing past the Faroe Islands, *ICES CM 1994/S*, *4*, 1–16, 1994.
Hansen, B., and S. Østerhus, North Atlantic–Nordic Seas exchanges, *Prog. Oceanogr.*, *45*(2), 109–208, doi:10.1016/S0079-6611(99)00052-X, 2000.
Hansen, B., W. R. Turrell, and S. Østerhus, Decreasing overflow from the Nordic Seas into the Atlantic Ocean through the Faroe Bank Channel since 1950, *Nature*, *411*(6840), 927–930, doi:10.1038/35082034, 2001.
Hansen, B., S. Østerhus, H. Hátún, R. Kristiansen, and K. M. H. Larsen, The Iceland-Faroe inflow of Atlantic water to the Nordic Seas, *Prog. Oceanogr.*, *59*(4), 443–474, doi:10.1016/j.pocean.2003.10.003, 2003.
Hilmer, M., and T. Jung, Evidence for a recent change in the link between the North Atlantic Oscillation and Arctic sea ice export, *Geophys. Res. Lett.*, *27*(7), 989–992, doi:10.1029/1999GL010944, 2000.
Hoerling, M., J. Hurrell, T. Xu, G. Bates, and A. Phillips, Twentieth century north atlantic climate change. part II: Understanding the effect of indian ocean warming, *Clim. Dynam.*, *23*(3-4), 391–405, doi:10.1007/s00382-004-0433-x, 2004.
Hoerling, M. P., J. W. Hurrell, and T. Y. Xu, Tropical origins for recent North Atlantic climate change, *Science*, *292*(5514), 90–92, doi:10.1126/science.1058582, 2001.
Holliday, N. P., R. T. Pollard, J. F. Read, and H. Leach, Water mass properties and fluxes in the Rockall Trough, 1975–1998, *Deep-Sea Res. I*, *47*(7), 1303–1332, doi:10.1016/S0967-0637(99)00109-0, 2000.
Hurrell, J., Decadal trends in the North Atlantic Oscillation: Regional temperatures and precipitation, *Science*, *269*(5224), 676–679, 1995.
Hurrell, J., M. Hoerling, A. Phillips, and T. Xu, Twentieth century north atlantic climate change. part I: Assessing determinism, *Clim. Dynam.*, doi:10.1007/s00382-004-0432-y, 2004.
Hurrell, J. W., Y. Kushnir, G. Ottersen, and M. Visbeck, An overview of the North Atlantic Oscillation, in *The North Atlantic Oscillation: Climatic Significance and Environmental Impact*, *Geophysical Monograph Series*, vol. 134, edited by J. W. Hurrell, Y. Kushnir, G. Ottersen, and M. Visbeck, pp. 1–36, AGU, doi:10.1029/134GM01, 2003.
Jakobsen, P., M. Ribergaard, D. Quadfasel, T. Schmith, and C. Hughes, Near-surface circulation in the northern North Atlantic as inferred from Lagrangian drifters: Variability from the mesoscale to interannual, *J. Geophys. Res.*, *108*(C8), 3251, doi:10.1029/2002JC001554, 2003.
Johannessen, O. M., E. V. Shalina, and M. Miles, Satellite evidence for an Arctic sea ice cover in transformation, *Science*, *286*(5446), 1937–1939, doi:10.1126/science.286.5446.1937, 1999.
Johannessen, O. M., et al., Arctic climate change: Observed and modelled temperature and sea-ice variability, *Tellus*, *56A*(4), 328–341, doi:10.1111/j.1600-0870.2004.00060.x, 2004.
Jones, P. D., T. Jonsson, and D. Wheeler, Extension to the North Atlantic Oscillation using early instrumental pressure observations from Gibraltar and South-West Iceland, *Int. J. Climatol.*, *17*(13), 1433–1450, doi:10.1002/(SICI)1097-0088(19971115)17:13<1433::AID-JOC203>3.0.CO;2-P, 1997.
Josey, S., A comparison of ECMWF, NCEP–NCAR, and SOC surface heat fluxes with moored buoy measurements in the subduction region of the northeast Atlantic, *J. Climate*, *14*(8), 1780–1789, doi:10.1175/1520-0442(2001)014<1780:ACOENN>2.0.CO;2, 2001.
Jung, T., and M. Hilmer, The link between the North Atlantic Oscillation and Arctic Sea ice export through Fram Strait, *J. Climate*, *14*(19), 3932–3943, doi:10.1175/1520-0442(2001)014<3932:TLBTNA>2.0.CO;2, 2001.
Kalnay, E., et al., The NCEP/NCAR 40-year reanalysis project, *Bull. Am. Met. Soc.*, *77*(3), 437–471, doi:10.1175/1520-0477(1996)077<0437:TNYRP>2.0.CO;2, 1996.
Karcher, M. J., R. Gerdes, F. Kauker, and C. Köberle, Arctic warming: Evolution and spreading of the 1990s warm event in the Nordic Seas and the Arctic Ocean, *J. Geophys. Res.*, *108*(C2), 3034, doi:10.1029/2001JC001265, 2003.

Kindem, I. K. T., and B. Christiansen, Tropospheric response to stratospheric ozone loss, *Geophys. Res. Lett.*, *28*(8), 1547–1550, doi:10.1029/2000GL012552, 2001.

Kistler, R., et al., The NCEP-NCAR 50-year reanalysis: Monthly means CD-ROM and documentation, *Bull. Am. Met. Soc.*, *82*(2), 247–268, doi:10.1175/1520-0477(2001)082<0247:TNNYRM>2.3.CO;2, 2001.

Kuzmina, S. I., O. M. Johannessen, L. Bengtson, H. Drange, L. P. Bobylev, and O. G. Aniskina, The north atlantic oscillation variability and change under anthropogenic forcing, *Geophys. Res. Lett.*, submitted., 2004.

Kvamstø, N. G., P. Skeie, and D. B. Stephenson, Impact of Labrador sea-ice extent on the North Atlantic oscillation, *Int. J. Climatol.*, *24*(5), 603–612, doi:10.1002/joc.1015, 2004.

Kwok, R., G. F. Cunningham, and S. S. Pang, Fram Strait sea ice outflow, *J. Geophys. Res.*, *109*(C1), C01009, doi:10.1029/2003JC001785, 2004.

Levitus, S., J. I. Antonov, T. P. Boyer, and C. Stephens, Warming of the world ocean, *Science*, *287*(5461), 2225–2229, doi:10.1126/science.287.5461.2225, 2000.

Magnusdottir, G., C. Deser, and R. Saravanan, The effects of north atlantic sst and sea ice anomalies on the winter circulation in CCM3. part i: Main features and storm track characteristics of the response, *J. Climate*, *17*(5), 857–876, doi:10.1175/1520-0442(2004)017, 2004.

Marshall, J., H. Johnson, and J. Goodman, A study of the interaction of the North Atlantic Oscillation with the ocean circulation, *J. Climate*, *14*(7), 1399–1421, doi:10.1175/1520-0442(2001)014<1399:ASOTIO>2.0.CO;2, 2001a.

Marshall, J., Y. Kushnir, D. Battisti, P. Chang, A. Czaja, R. Dickson, M. McCartney, R. Saravanan, and M. Visbeck, North Atlantic climate variability: Phenomena, impacts and mechanisms, *Int. J. Climatol.*, *21*(15), 1863–1898, doi:10.1002/joc.693, 2001b.

Meincke, J., B. Rudels, and H. Friedrich, The Arctic Ocean–Nordic Seas thermohaline system, *ICES J. Mar. Sci.*, *54*(3), 283–299, doi:10.1006/jmsc.1997.0229, 1997.

Morison, J., M. Steele, and R. Andersen, Hydrography of the upper Arctic Ocean measured from the nuclear submarine U.S.S. Pargo, *Deep-Sea Res. I*, *45*(1), 15–38, doi:10.1016/S0967-0637(97)00025-3, 1998.

Mork, K. A., and J. Blindheim, Variation in the Atlantic Inflow to the Nordic Seas, 1955–1996, *Deep-Sea Res. I*, *47*(6), 1035–1057, doi:10.1016/S0967-0637(99)00091-6, 2000.

Nilsen, J. E. Ø., and E. Falck, Variations of mixed layer depth and water properties in the Norwegian Sea during 50 years, *Prog. Oceanogr.*, submitted, 2004.

Nilsen, J. E. Ø., Y. Gao, H. Drange, T. Furevik, and M. Bentsen, Simulated North Atlantic–Nordic Seas water mass exchanges in an isopycnic coordinate OGCM, *Geophys. Res. Lett.*, *30*(10), 1536, doi:10.1029/2002GL016597, 2003.

Nobre, P., and J. Srukla, Variations of sea surface temperature, wind stress, and rainfall over the tropical Atlantic and South America, *J. Climate*, *9*(10), 2464–2479, doi:10.1175/1520-0442(1996)009<2464:VOSSTW>2.0.CO;2, 1996.

Nøst, O. A., and P. E. Isachsen, The large-scale time-mean ocean circulation in the Nordic Seas and Arctic Ocean estimated from simplified dynamics, *J. Mar. Res.*, *61*(2), 175–210, doi:10.1357/002224003322005069, 2003.

Orvik, K. A., The deepening of the Atlantic Water in the Lofoten Basin of the Norwegian Sea, demonstrated by using an active reduced gravity model, *Geophys. Res. Lett.*, *31*, L01306, doi:10.1029/2003GL018687, 2004.

Orvik, K. A., and P. Niiler, Major pathways of Atlantic water in the northern North Atlantic and Nordic Seas towards arctic, *Geophys. Res. Lett.*, *29*(19), 1896, doi:10.1029/2002GL015002, 2002.

Orvik, K. A., and Ø. Skagseth, Monitoring the Norwegian Atlantic Slope Current using a single moored current meter, *Cont. Shelf Res.*, *23*(2), 159–176, doi:10.1016/S0278-4343(02)00172-3, 2003a.

Orvik, K. A., and Ø. Skagseth, The impact of the wind stress curl in the North Atlantic on the Atlantic inflow to the Norwegian Sea toward the Arctic, *Geophys. Res. Lett.*, *30*(17), 1884, doi:10.1029/2003GL017932, 2003b.

Orvik, K. A., Ø. Skagseth, and M. Mork, Atlantic Inflow to the Nordic Seas. Current structure and volume fluxes from moored current meters, VM–ADCP and SeaSoar-CTD observations, 1995–1999, *Deep-Sea Res. I*, *48*(4), 937–957, doi:10.1016/S0967-0637(00)00038-8, 2001.

Østerhus, S., and T. Gammelsrød, The abyss of the Nordic Seas is warming, *J. Climate*, *12*(11), 3297–3304, doi:10.1175/1520-0442(1999)012<3297:TAOTNS>2.0.CO;2, 1999.

Peterson, K. A., R. J. Greatbatch, J. Lu, H. Lin, and J. Derome, Hindcasting the NAO using diabatic forcing of a simple AGCM, *Geophys. Res. Lett.*, *29*(9), doi:10.1029/2001GL014502, 2002.

Portis, D. H., J. E. Walsh, M. E. Hamly, and P. J. Lamb, Seasonality of the North Atlantic Oscillation, *J. Climate*, *14*(9), 2069–2078, doi:10.1175/1520-0442(2001)014<2069:SOTNAO>2.0.CO;2, 2001.

Poulain, P.-M., A. Warn-Varnas, and P. Niiler, Near surface circulation of the Nordic Seas as measured by lagrangian drifters, *J. Geophys. Res.*, *101*(C8), 18,237–18,258, doi:10.1029/96JC00506, 1996.

Quadfasel, D., J.-C. Gascard, and K.-P. Koltermann, Large-scale oceanography in Fram Strait during the 1984 Marginal Ice Zone Experiment, *J. Geophys. Res.*, *92*(C7), 6719–6728, 1987.

Rahmstorf, S., and A. Ganopolski, Long-term global warming scenarios computed with an efficient coupled climate model, *Climatic Change*, *43*(2), 353–367, doi:10.1023/A:1005474526406, 1999.

Reynolds, R., and T. Smith, Improved global sea surface temperature analyses, *J. Climate*, *7*(6), 929–948, doi:710.1175/1520-0442(1994)007<0929:IGSSTA>2.0.CO;2, 1994.

Rodwell, M., D. Rowell, and C. K. Folland, Oceanic forcing of the wintertime North Atlantic Oscillation and European climate, *Nature*, *398*(6725), 320–323, doi:10.1038/18648, 1999.

Rogers, J. C., The association between the North Atlantic Oscillation and the Southern Oscillation in the northern hemisphere, *Mon. Weather Rev.*, *112*(10), 1999–2015, doi:10.1175/1520-0493(1984)112<1999:TABTNA>2.0.CO;2, 1984.

Rothrock, D. A., Y. Yu, and G. A. Maykut, Thinning of the Arctic sea-ice cover, *Geophys. Res. Lett.*, *26*(23), 3469–3472, doi:10.1029/1999GL010863, 1999.

Rothrock, D. A., J. Zhang, and Y. Yu, The Arctic ice thickness anomaly of the 1990s: A consistent view from observations and models, *J. Geophys. Res.*, *108*(C3), 3083, doi:10.1029/2001JC001208, 2003.

Schmith, T., and C. Hansen, Fram Strait ice export during the nineteenth and twentieth centuries reconstructed from a multiyear sea ice index from southwestern Greenland, *J. Climate*, *16*(16), 2782–2791, doi:10.1175/1520-0442(2003)016<2782:FSIEDT>2.0.CO;2, 2003.

Serreze, M., et al., A record minimum Arctic Sea ice extent and area in 2002, *Geophys. Res. Lett.*, *30*(3), doi:10.1029/2002GL016406, 2003.

Serreze, M. C., and C. M. Hurst, Representation of mean Arctic precipitation from NCEP–NCAR and ERA reanalysis, *J. Climate*, *13*(1), 182–201, doi:10.1175/1520-0442(2000)013<0182:ROMAPF>2.0.CO;2, 2000.

Shindell, D. T., R. L. Miller, G. A. Schmidt, and L. Pandolfo, Simulation of recent northern winter climate trends by greenhouse-gas forcing, *Nature*, *399*(6735), 452–455, doi:10.1038/20905, 1999.

Simonsen, K., and P. Haugan, Heat budgets of the arctic mediterranean and sea surface heat flux parameterizations for the nordic seas, *J. Geophys. Res.*, *101*(C3), 6553–6576, doi:10.1029/95JC03305, 1996.

Skagseth, Ø., K. A. Orvik, and T. Furevik, Coherent variability of the Norwegian Atlantic Slope Current derived from TOPEX/ERS altimeter data, *Geophys. Res. Lett.*, *31*(14), L14304, doi:10.1029/2004GL020057, 2004.

Steele, M., R. Morley, and W. Ermold, PHC: A global ocean hydrography with a high-quality Arctic Ocean, *J. Climate*, *14*(9), 2079–2087, doi:10.1175/1520-0442(2001)014<2079:PAGOHW>2.0.CO;2, 2001.

Stephenson, D. B., and V. Pavan, The North Atlantic Oscillation in coupled climate models: A CMIP1 evaluation, *Clim. Dynam.*, *20*(4), 381–399, doi:10.1007/s00382-002-0281-5, 2003.

Stephenson, D. B., V. Pavan, and R. Bojaril, Is the North Atlantic Oscillation a random walk?, *Int. J. Climatol.*, *20*(1), 1–18, doi:10.1002/(SICI)1097-0088(200001)20:1<1::AID-JOC456>3.0.CO;2-P, 2000.

Stephenson, D. B., H. Wanner, S. Brönnimann, and J. Luterbacher, The history of scientific research on the North Atlantic Oscillation, in *The North Atlantic Oscillation: Climatic Significance and Environmental Impact*, *Geophysical Monograph Series*, vol. 134, edited by J. W. Hurrell, Y. Kushnir, G. Ottersen, and M. Visbeck, pp. 37–50, AGU, doi:10.1029/134GM02, 2003.

Stigebrandt, A., A model for the thickness and salinity of the upper layer in the Arctic Ocean and the relationship between the ice thickness and some external parameters, *J. Phys. Oceanogr.*, *11*(10), 1407–1422, doi:10.1175/1520-0485(1981)011<1407:AMFTTA>2.0.CO;2, 1981.

Sutton, R. T., S. P. Jewson, and D. P. Rowell, The elements of climate variability in the tropical Atlantic region, *J. Climate*, *13*(18), 3261–3284, doi:10.1175/1520-0442(2000)013<3261:TEOCVI>2.0.CO;2, 2000.

Sverdrup, H. U., Wind driven currents in a baroclinic ocean; with application to the equatorial currents of the eastern pacific, *Proceedings, National Academy of Science, Washington*, *33*, 318–326, 1947.

Swift, J. H., E. P. Jones, K. Aagaard, E. C. Carmack, M. Hingston, R. W. MacDonald, F. A. McLaughlin, and R. G. Perkin, Waters of the Makarov and Canada basins, *Deep-Sea Res. II*, *44*(8), 1503–1529, doi:10.1016/S0967-0645(97)00055-6, 1997.

Thompson, D. W., and J. M. Wallace, The Arctic Oscillation signature in the wintertime geopotential height and temperature fields, *Geophys. Res. Lett.*, *25*(9), 1297–1300, doi:10.1029/98GL00950, 1998.

Thompson, D. W. J., and J. M. Wallace, Annular modes in the extratropical circulation. part I: Month-to-month variability, *J. Climate*, *13*(5), 1000–1016, doi:10.1175/1520-0442(2000)013<1000:AMITEC>2.0.CO;2, 2000.

Thompson, D. W. J., S. Lee, and M. P. Baldwin, Atmospheric processes governing the Northern Hemisphere Annular Mode/North Atlantic Oscillation, in *The North Atlantic Oscillation: Climatic Significance and Environmental Impact*, *Geophysical Monograph Series*, vol. 134, edited by J. W. Hurrell, Y. Kushnir, G. Ottersen, and M. Visbeck, pp. 81–112, AGU, doi:10.1029/134GM05, 2003.

Turrell, W., B. Hansen, S. Hughes, and S. Østerhus, Hydrographic variability during the decade of the 1990's in the northeast Atlantic and southern Norwegian Sea, in *Hydrobiological Variability in the ICES Area, 1990–99*, *ICES Mar. Sci. Symp.*, vol. 219, edited by W. Turrell, A. Lavín, K. F. Drinkwater, M. St. John, and J. Watson, pp. 111–120, ICES, 2003.

Turrell, W. R., G. Slesser, R. D. Adams, R. Payne, and P. A. Gillibrand, Decadal variability in the composition of Faroe Shetland Channel bottom water, *Deep-Sea Res. I*, *46*(1), 1–25, doi:10.1016/S0967-0637(98)00067-3, 1999.

Ulbrich, U., and M. Christoph, A shift of the nao and increasing storm track activity over europe due to anthropogenic greenhouse gas forcing, *Clim. Dynam.*, *15*(7), 551–559, doi:10.1007/s003820050299, 1999.

Vikebø, F., T. Furevik, G. Furnes, N. G. Kvamstø, and M. Reistad, Wave height variations in the North Sea

and on the Norwegian Continental Shelf 1881–1999, *Cont. Shelf Res.*, *23*(3-4), 251–263, doi:10.1016/S0278-4343(02)00210-8, 2003.

Vinje, T., Fram Strait ice fluxes and atmospheric circulation: 1950–2000, *J. Climate*, *14*(16), 3508–3517, doi:10.1175/1520-0442(2001)014<3508:FSIFAA>2.0.CO;2, 2001.

Vinje, T., N. Nordlund, and Å. Kvambekk, Monitoring ice thickness in Fram Strait, *J. Geophys. Res.*, *103*(C5), doi:10.1029/97JC03360, 1998.

Visbeck, M., E. P. Chassignet, R. Curry, T. Delworth, B. Dickson, and G. Krahmann, The ocean's response to North Atlantic Oscillation variability, in *The North Atlantic Oscillation: Climatic Significance and Environmental Impact*, *Geophysical Monograph Series*, vol. 134, edited by J. W. Hurrell, Y. Kushnir, G. Ottersen, and M. Visbeck, pp. 113–145, AGU, doi:10.1029/134GM06, 2003.

von Storch, H., Spatial patterns: EOFs and CCA, in *Analysis of Climate Variability*, edited by H. von Storch and A. Navarra, chap. 13, Springer, 1995.

Watson, A., et al., Mixing and convection in the Greenland Sea from a tracer-releaease experiment, *Nature*, *401*(6756), 902–904, doi:10.1038/44807, 1999.

Widell, K., S. Østerhus, and T. Gammelsrød, Sea ice velocity in the Fram Strait monitored by moored instruments, *Geophys. Res. Lett.*, *30*(19), 1982, doi:10.1029/2003GL018119, 2003.

Willebrand, J., S. Philander, and R. Pacanowski, The oceanic response to large-scale atmospheric disturbances, *J. Phys. Oceanogr.*, *10*(3), 411–429, doi:10.1175/1520-0485(1980)010<0411:TORTLS>2.0.CO;2, 1980.

Wu, P., R. Wood, and P. Stott, Does the recent freshening trend in the North Atlantic indicate a weakening thermohaline circulation?, *Geophys. Res. Lett.*, *31*(2), L02301, doi:10.1029/2003GL018584, 2004.

Zhang, J., D. A. Rothrock, and M. Steele, Warming of the Arctic Ocean by a strengthened Atlantic inflow: Model results, *Geophys. Res. Lett.*, *25*(10), 1745–1748, doi:10.1029/98GL01299, 1998.

Zhang, X., M. Ikeda, and J. E. Walsh, Arctic sea ice and freshwater changes driven by the atmospheric leading mode in a coupled sea ice-ocean model, *J. Climate*, *16*(13), 2159–2177, doi:10.1175/2758.1, 2003.

T. Furevik, Geophysical Institute, Allégt. 70, 5007 Bergen, Norway (email: tore@gfi.uib.no)

J. Even Ø. Nilsen, Nansen Environmental and Remote Sensing Center, Thormøhlensgt. 47, 5006 Bergen, Norway (email: even@nersc.no)

[1]Also at Bjerknes Centre for Climate Research, Bergen, Norway

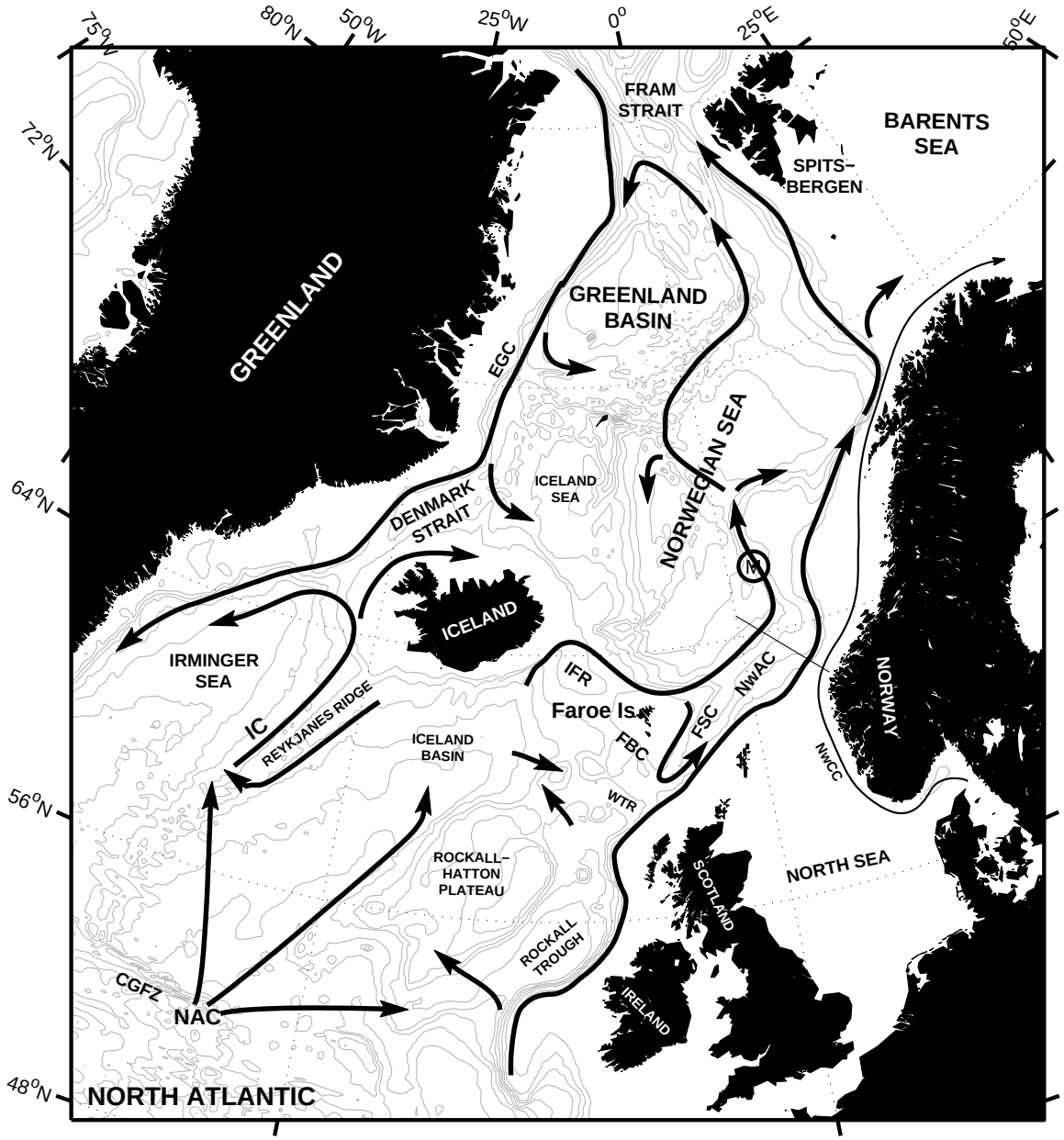

Figure 1. The northern North Atlantic and the Nordic Seas. Isobaths are drawn for every 500 m. Schematic surface currents are based on literature [*Poulain et al.*, 1996; *Hansen and Østerhus*, 2000; *Bower et al.*, 2000; *Mork and Blindheim*, 2000; *Holliday et al.*, 2000; *Orvik et al.*, 2001; *Orvik and Niiler*, 2002; *Jakobsen et al.*, 2003]. See text for abbreviations. Circled M shows the position of Ocean Weather Station M and thin line indicates the Svinøy Section.

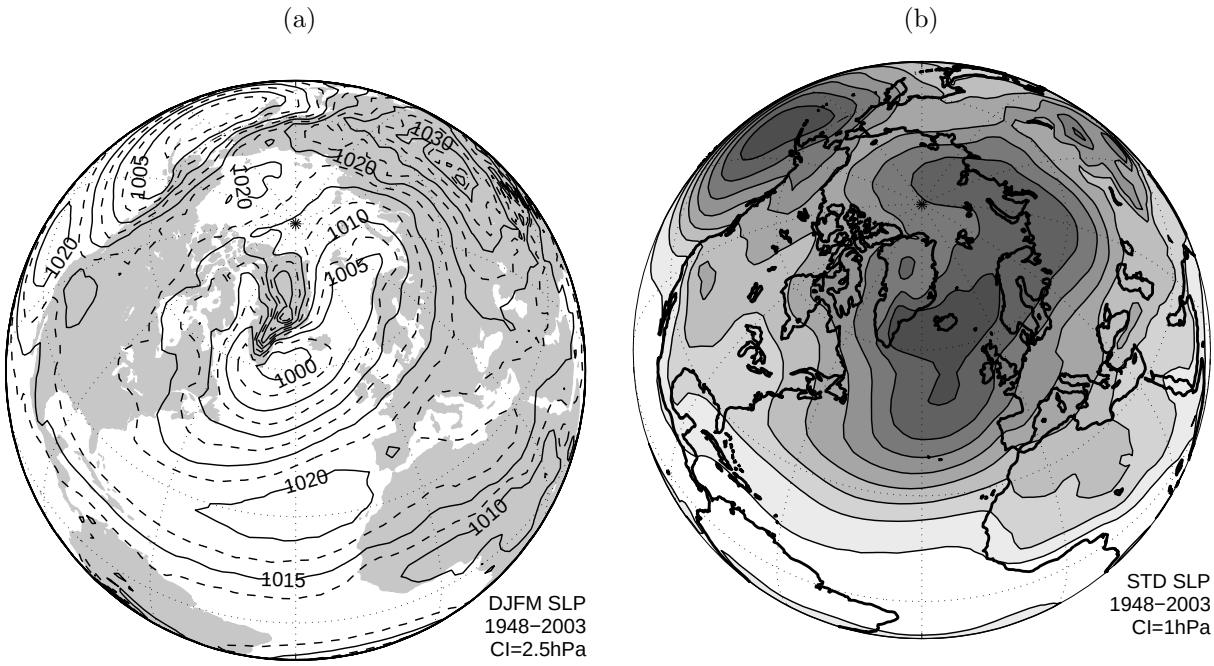

Figure 2. Winter-mean (a) and year-to-year standard deviation of the winter-mean (b) SLP for December through March 1949–2003 calculated from the NCEP/NCAR reanalysis data [*Kalnay et al.*, 1996]. Contour intervals (CI) are given at the lower right hand side of each plot. White colouring in (b) indicates values below 1 hPa.

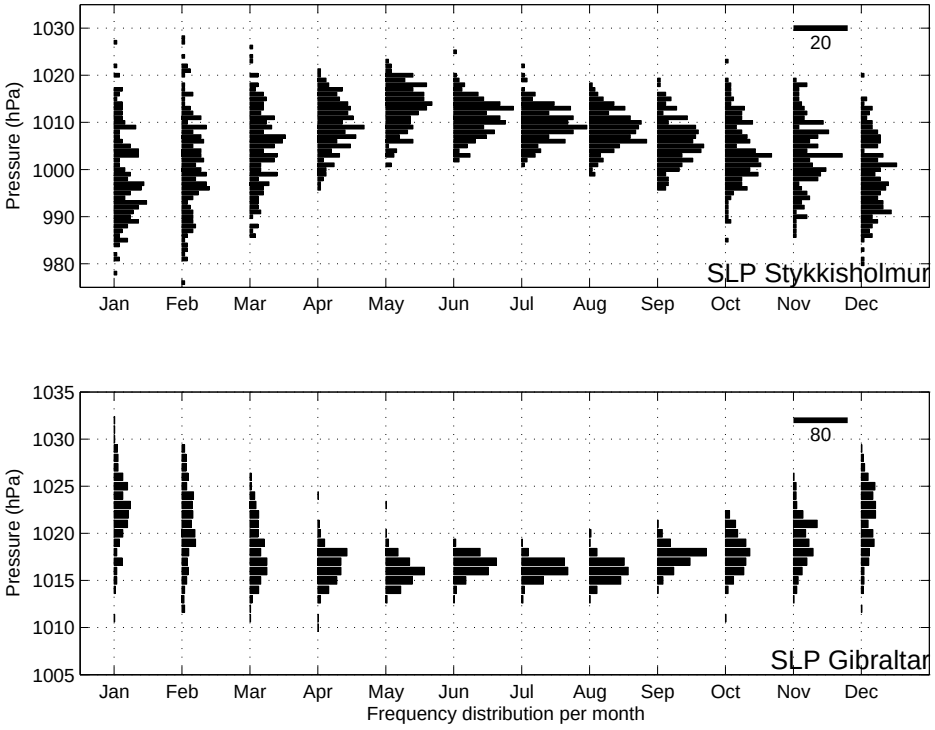

Figure 3. Frequency distribution of monthly-mean SLP for Stykkisholmur (upper) and Gibraltar (lower). For a given month, the number of years with the monthly-mean SLP inside each 1 hPa interval is shown. Note that the scales for SLP and for the frequency distribution (indicated in the upper right corner of each plot) differ. The plot is based on monthly-mean SLP data 1821–2000 provided by Phil Jones, Climatic Research Unit (CRU), University of East Anglia.

(a)

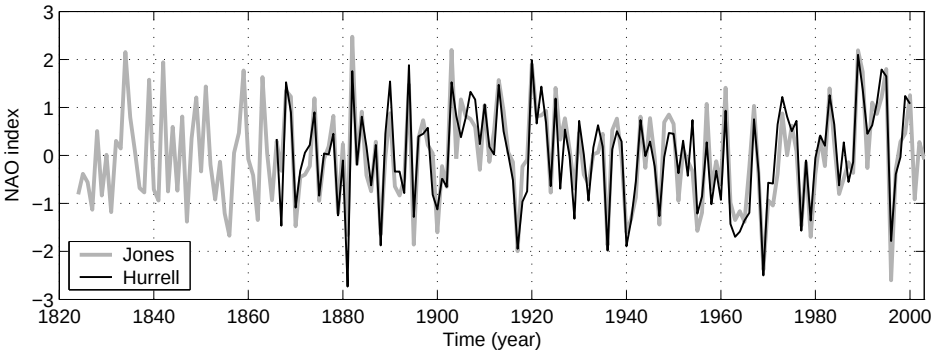

(b)

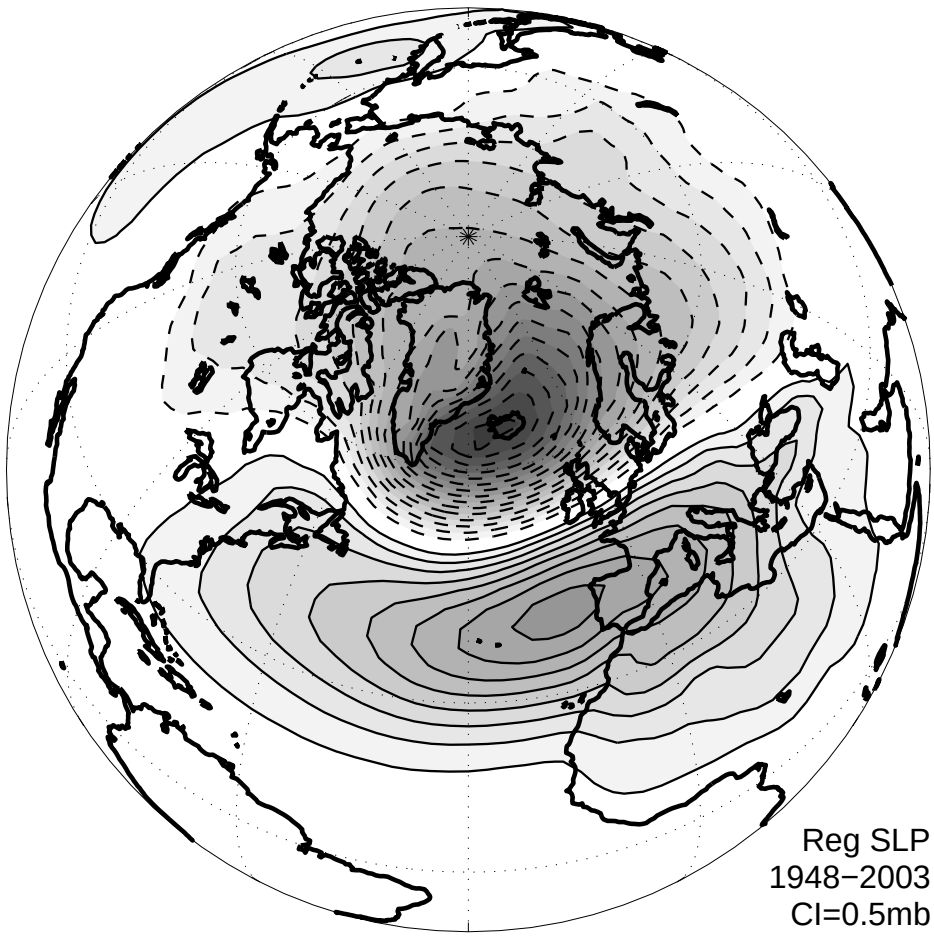

Figure 4. (a) The NAO winter-mean (Dec–Mar) indices calculated from the Gibraltar-Stykkisholmur (Jones' index, gray) and Lisbon-Stykkisholmur (Hurrell's index, black) SLP differences. (b) Monthly-mean SLP regressed on the standardized monthly-mean Jones index for the period December 1948 to March 2003. Only winter months (Dec–Mar) are used. The values correspond to a unit change in the Jones index. Solid lines are positive, dashed lines negative.

(a)

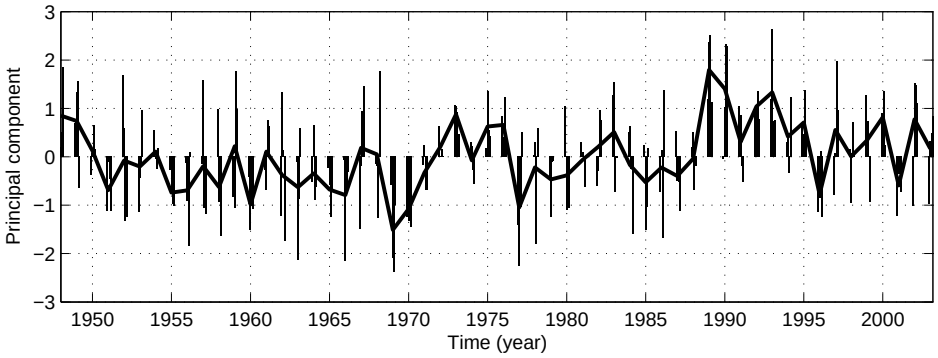

(b)

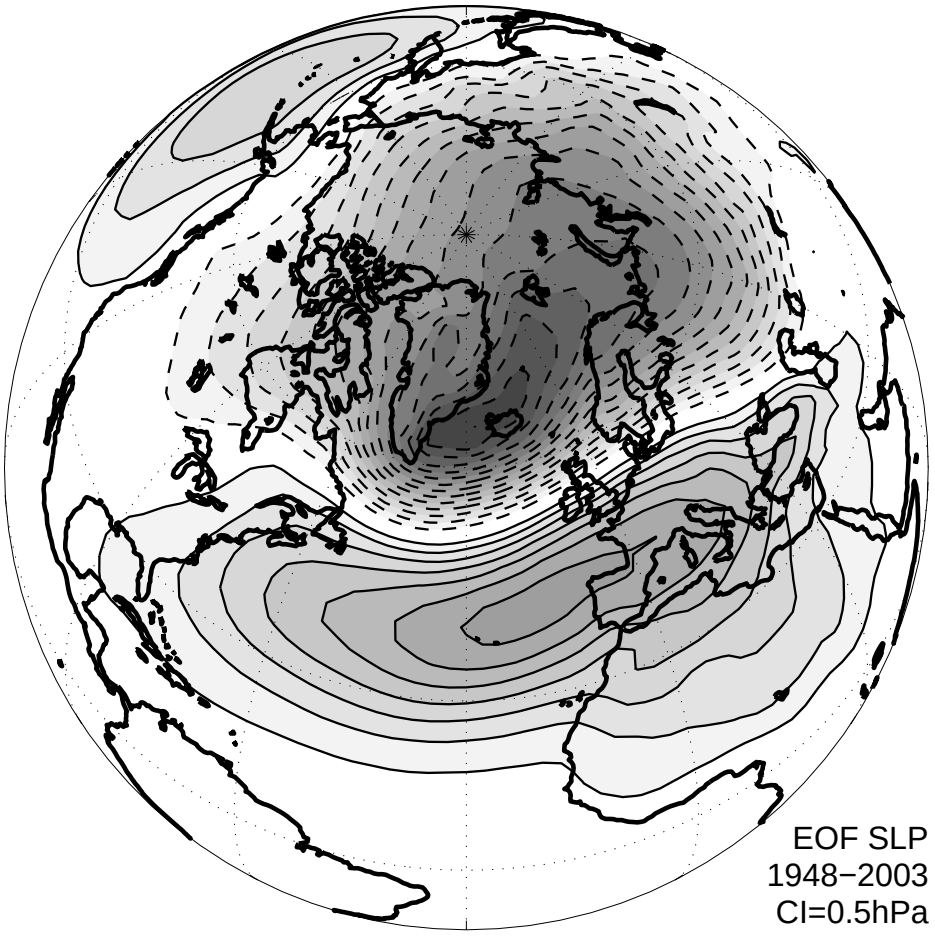

Figure 5. (a) The principal component of the leading mode of variability (1st EOF) of monthly-mean December through March SLP, defining the NAO-index used throughout the paper. The principal component is calculated from the 1948–2003 NCEP/NCAR reanalysis data for the Atlantic sector (90°W–30°E, 20°N–80°N). The monthly values are shown as bars, and the winter means are indicated by the thick line. (b) Winter monthly-mean SLP regressed on the principal component. Solid lines are positive, dashed lines negative.

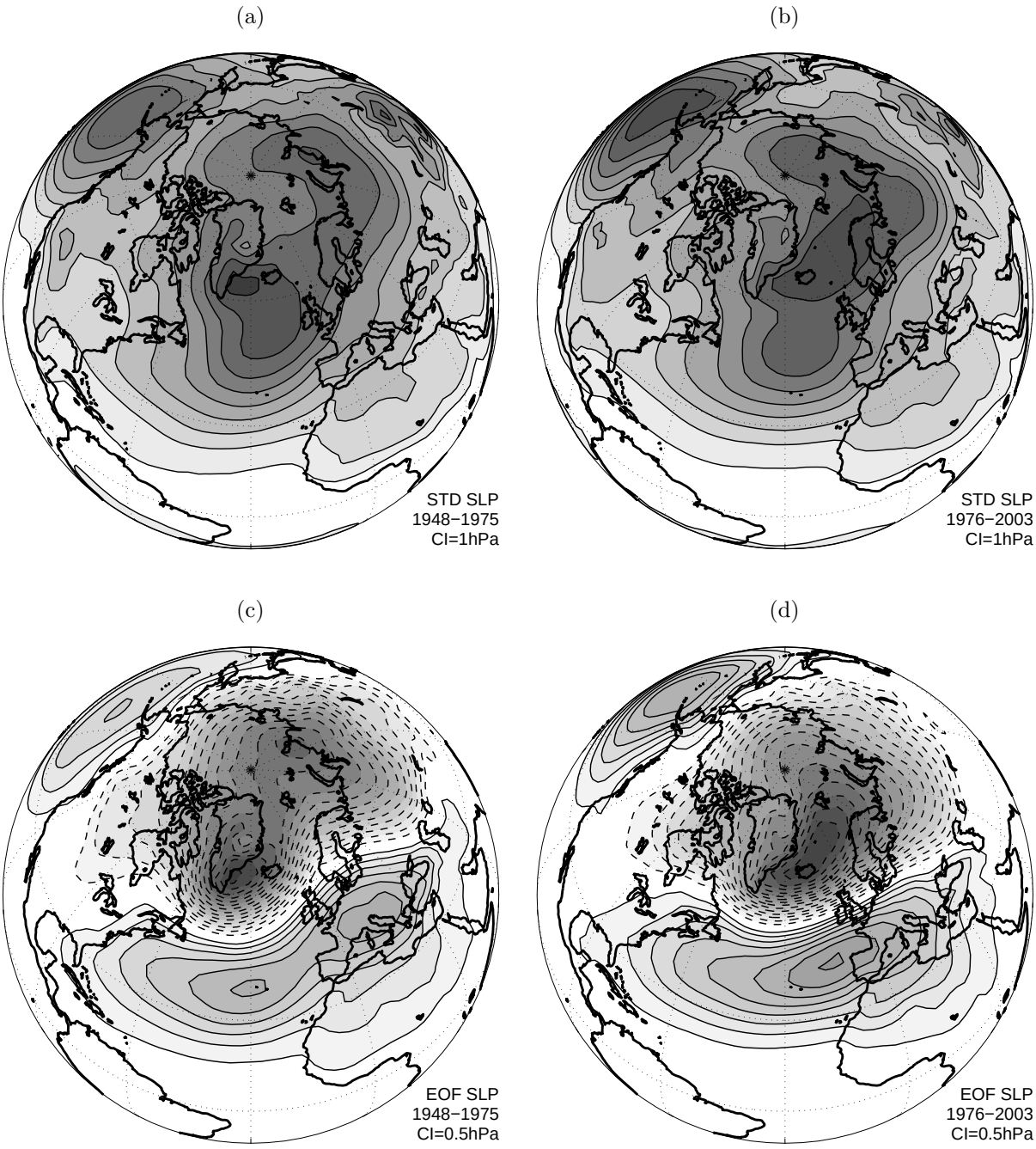

Figure 6. Standard deviation (upper panels) and the leading mode of variability (lower panels) of the winter-mean SLP for the periods 1948–1975 (left panels) and 1976–2003 (right panels). The principal components are calculated from the NCEP/NCAR reanalysis data for the Atlantic sector (90°W–30°E, 20°N–80°N). Solid lines are positive, dashed lines negative. White colouring in (a) and (b) indicates values below 1 hPa.

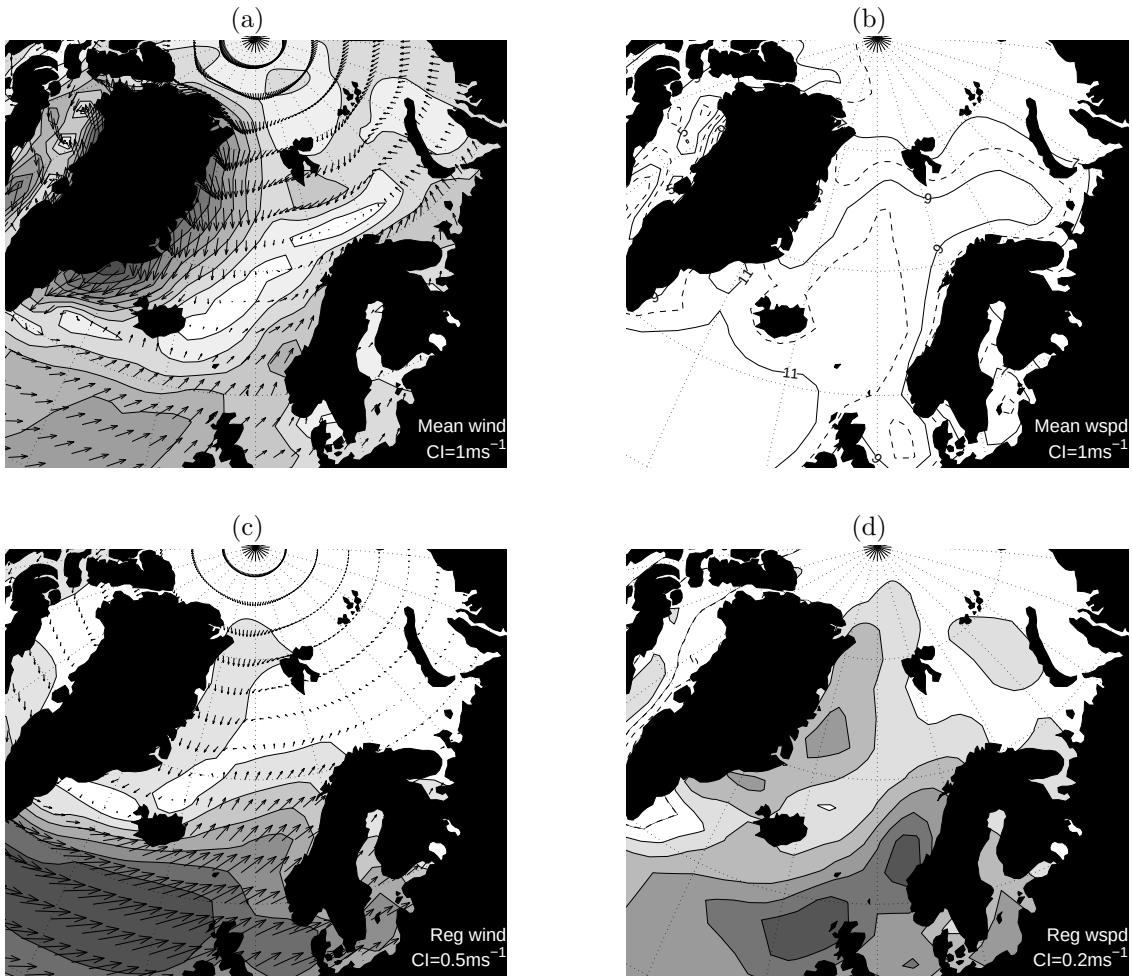

Figure 7. Winter-mean wind vectors with contours for magnitude (a) and winter-mean absolute wind speed (b) for the winters 1949–2003, and the regressions of these onto the NAO-index (c,d). The values correspond to a unit increase in the index. White colouring in (a,c,d) indicates values below 1, 0.5, or 0.2 ms^{-1} respectively.

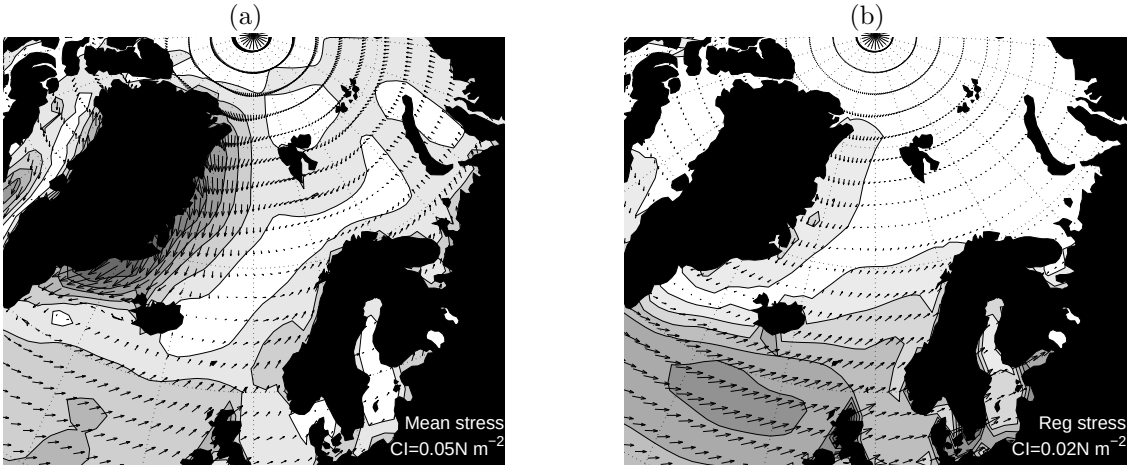

Figure 8. (a) Winter-mean wind stress and (b) the wind stress regressed on the NAO-index. The values correspond to a unit increase in the index. White colouring indicates values below 0.05 Nm^{-2} (a) or 0.02 Nm^{-2} (b).

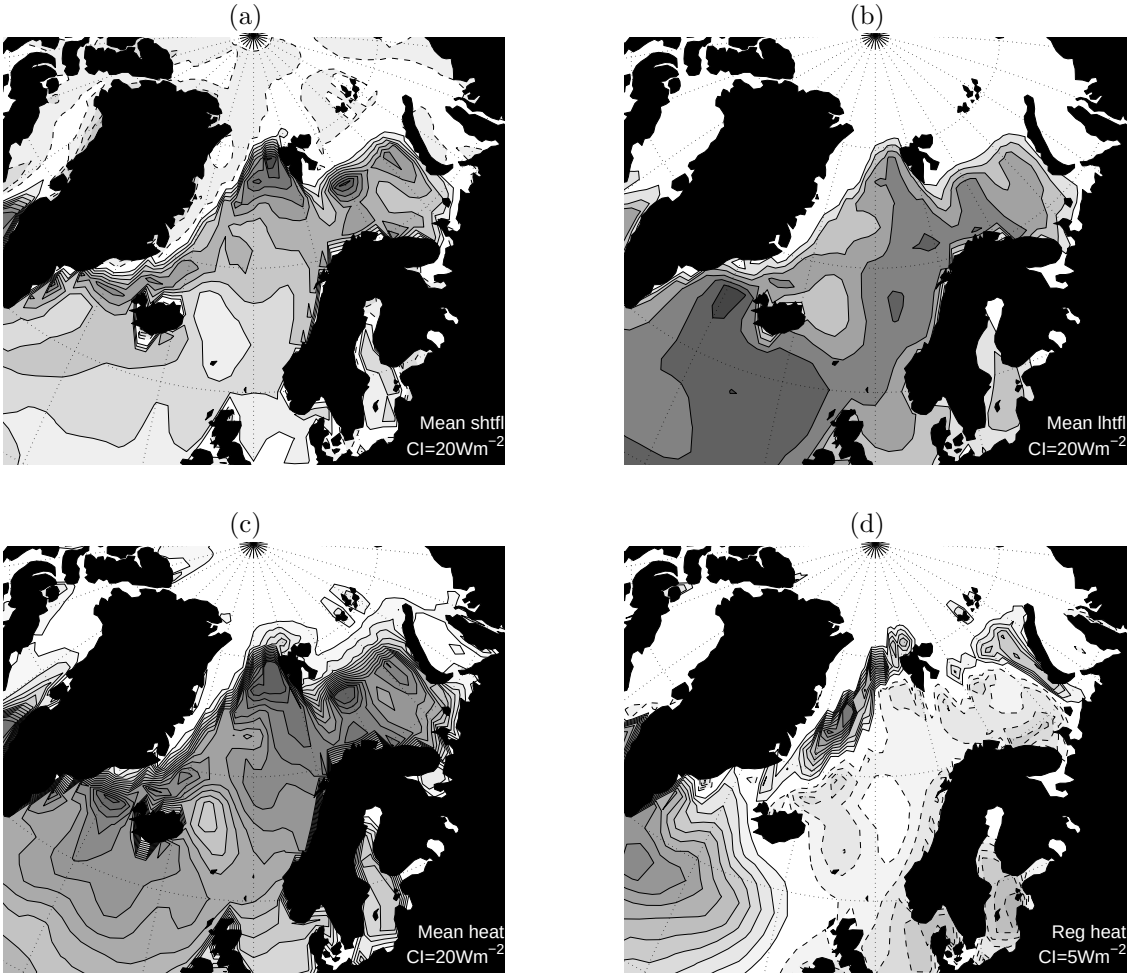

Figure 9. Winter-mean sensible heat flux (a), latent heat flux (b), total heat flux (c), and the total heat flux regressed on the NAO-index (d). Solid lines are positive (ocean temperatures will decrease), dashed lines negative.

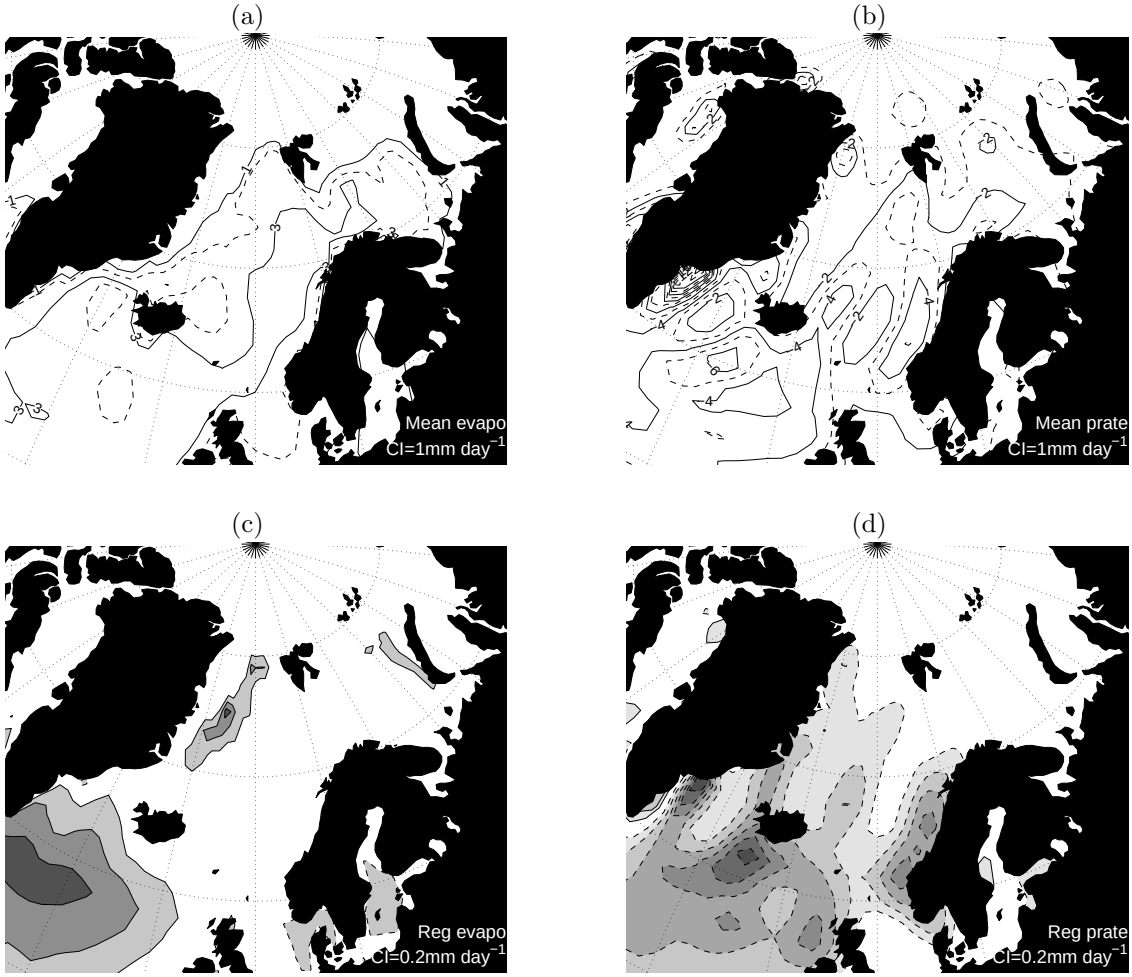

Figure 10. Winter-mean evaporation (a), precipitation (b), and the evaporation (c) and precipitation (d) regressed on the NAO-index. Solid lines are positive (ocean salinities will increase), dashed lines negative.

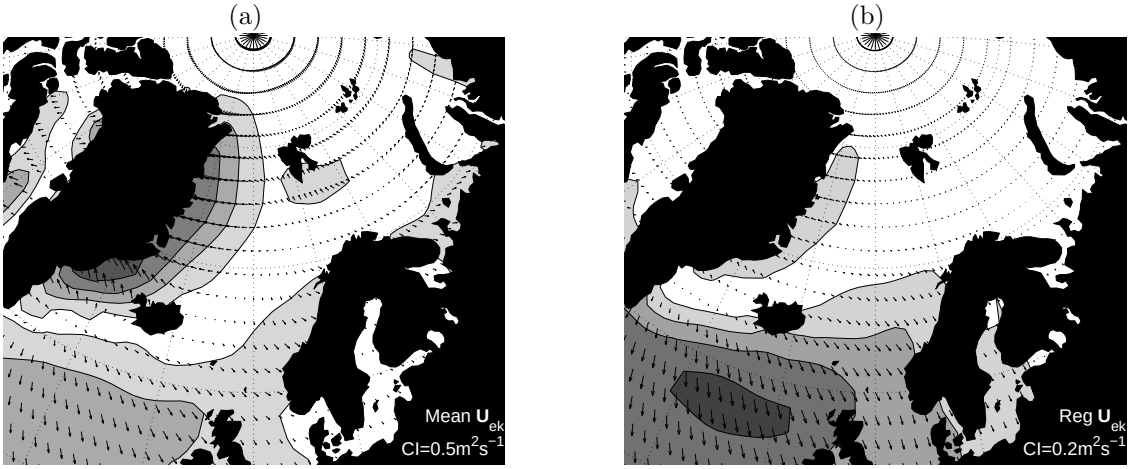

Figure 11. (a) Winter-mean Ekman volume transports and (b) the Ekman volume transports regressed on the NAO-index. The Ekman volume transports are calculated from the NCEP/NCAR reanalysis wind stress fields. Effects of sea-ice are ignored. White colouring indicates values below 0.5 m^2s^{-1} (a) or 0.2 m^2s^{-1} (b).

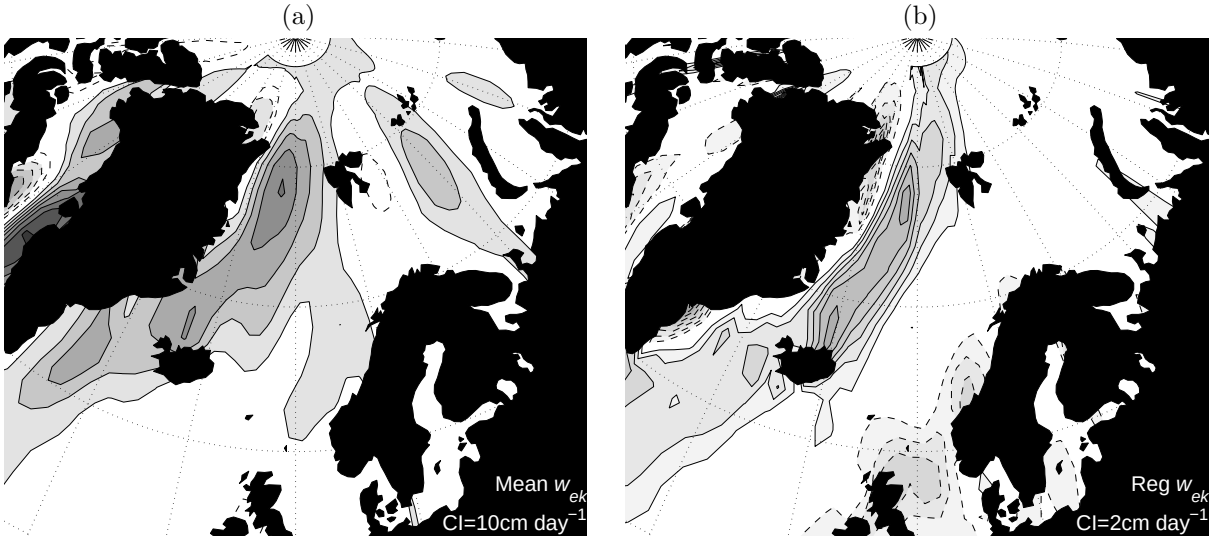

Figure 12. (a) Winter-mean Ekman pumping velocities and (b) the Ekman pumping velocities regressed on the NAO-index. The Ekman pumping velocities are calculated from the NCEP/NCAR reanalysis wind stress fields. Effects of sea-ice are ignored. Solid lines are positive, dashed lines negative. White colouring indicates values below 10 cm day^{-1} (a) or 2 cm day^{-1} (b).

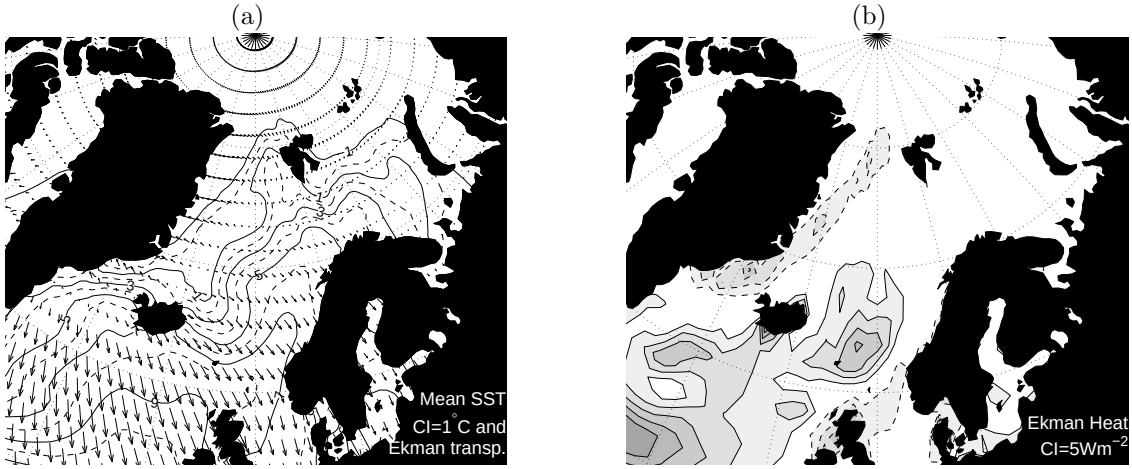

Figure 13. (a) Winter-mean SST field (contours) and anomalous Ekman transports (vectors) corresponding to the NAO-related wind stress anomalies (Figure 8b). (b) The heat divergence associated with the anomalous Ekman transports. Effects of sea-ice are ignored. Solid lines are positive (ocean temperatures will decrease), dashed lines negative. The SST data are updated from *Reynolds and Smith* [1994].

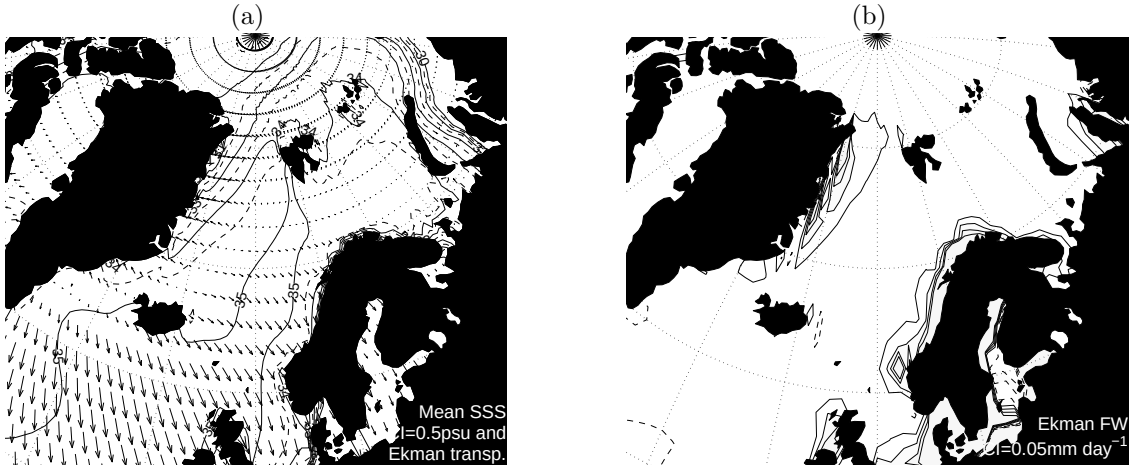

Figure 14. (a) Winter-mean SSS field (contours) and anomalous Ekman transports (vectors) corresponding to the NAO-related wind stress anomalies (Figure 8b). (b) The freshwater divergence associated with the anomalous Ekman transports. Effects of sea-ice are ignored. Solid lines are positive (ocean salinities will increase), dashed lines negative. The SSS data come from the Polar Science Center Hydrographical Climatology version 2.1, updated from *Steele et al.* [2001].

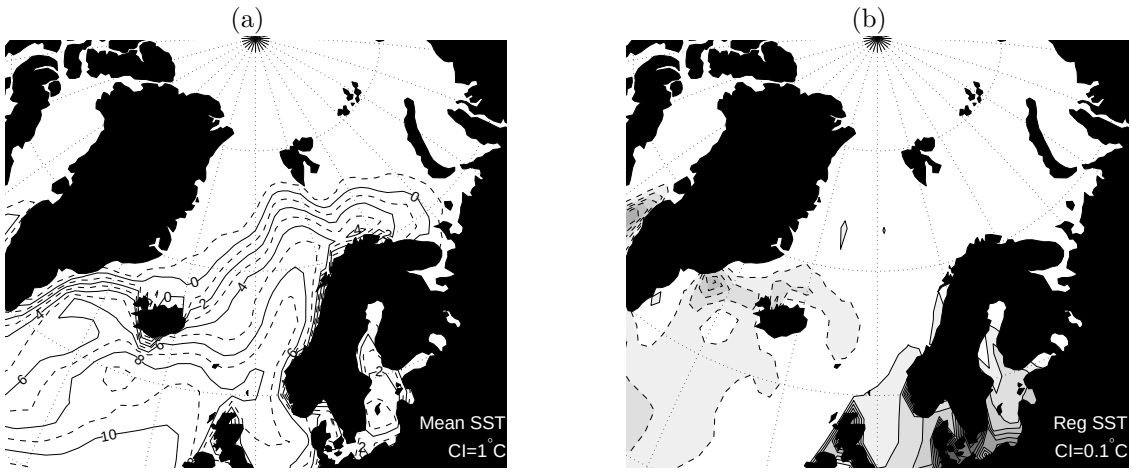

Figure 15. Winter-mean SST (a) and SST regressed on the NAO-index (b). In (b) solid lines are positive, dashed lines negative.

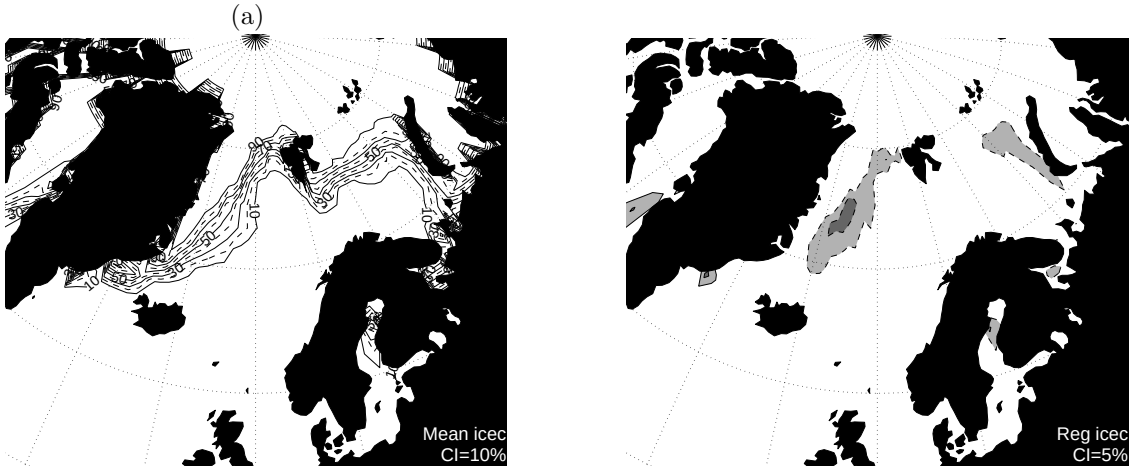

Figure 16. Winter-mean sea-ice concentration (a) and sea-ice concentration regressed on the NAO-index (b). In (b) solid lines are positive, dashed lines negative.

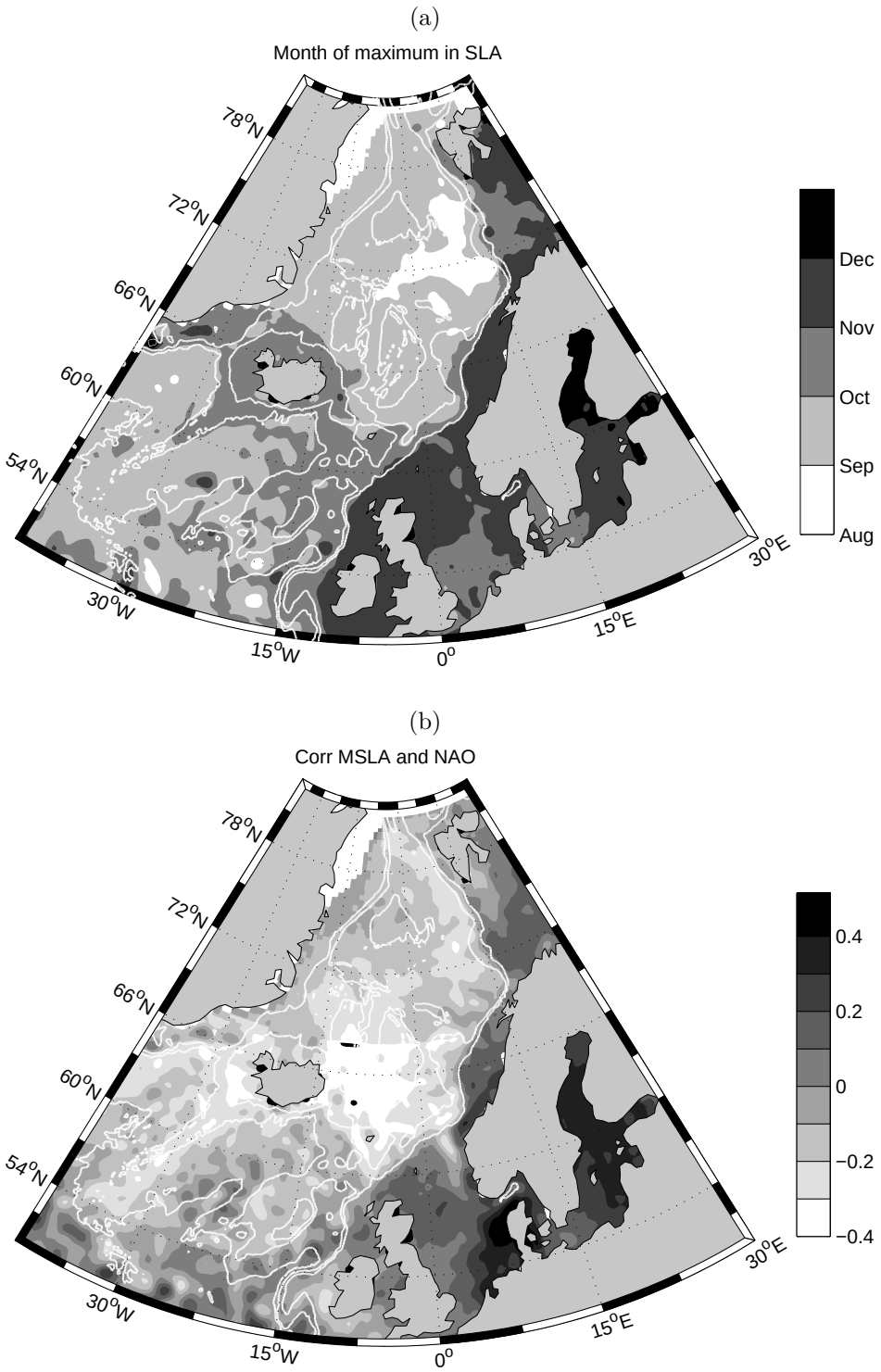

Figure 17. The combined Topex-Poseidon and ERS 1/2 sea-level anomaly (SLA). (a) The month of maximum climatological SLA, and (b) the SLA correlated with the Lisbon-Stykkisholmur (Hurrell) NAO-index. The monthly NAO-index has been interpolated to weekly values, and both the NAO and the SLA data have been deseasoned prior to the correlation. The white contours indicate f/H values corresponding to 500, 1500, and 3000 m depths at 60°N.

(a)

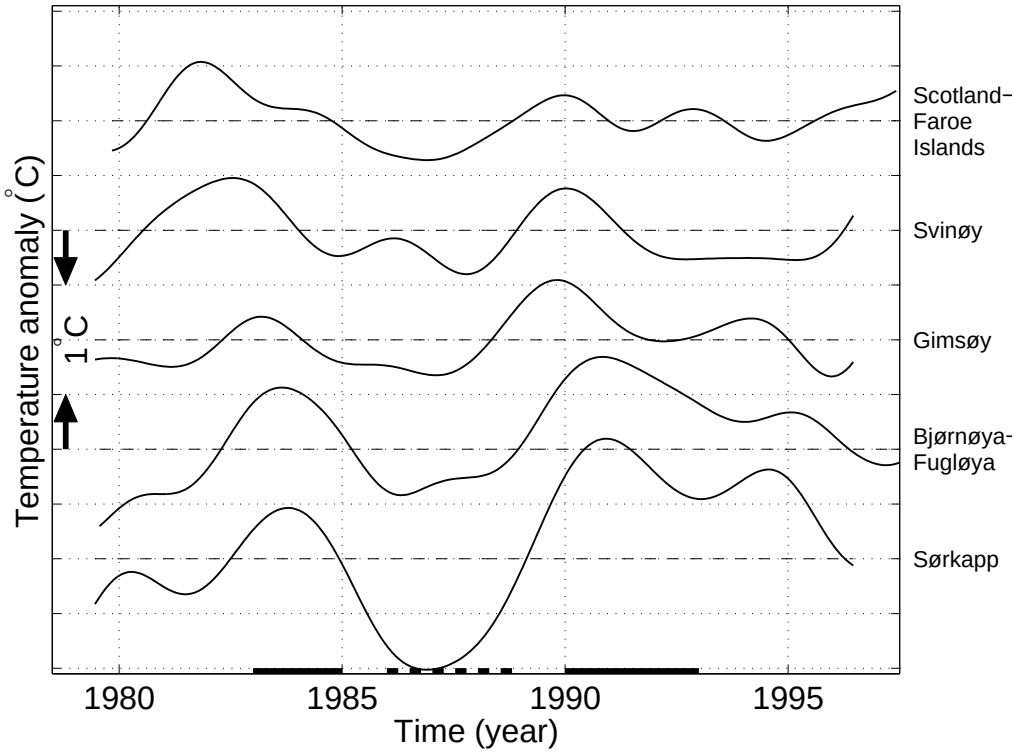

(b)

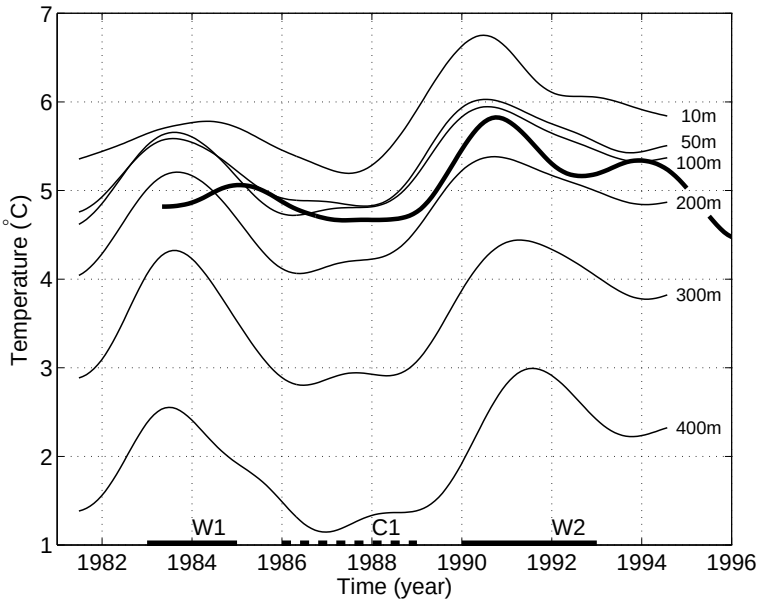

Figure 18. (a) Core temperatures in the flow of AW at five regular CTD (Conductivity Temperature Depth) sections from the FSC (upper curve) to the Southcape (76°N) Section (lower curve), and (b) average temperatures at the surface (bold curve) and at 6 different depths (thin curves) in the Barents Sea Opening. The figures are adapted from *Furevik* [2001].

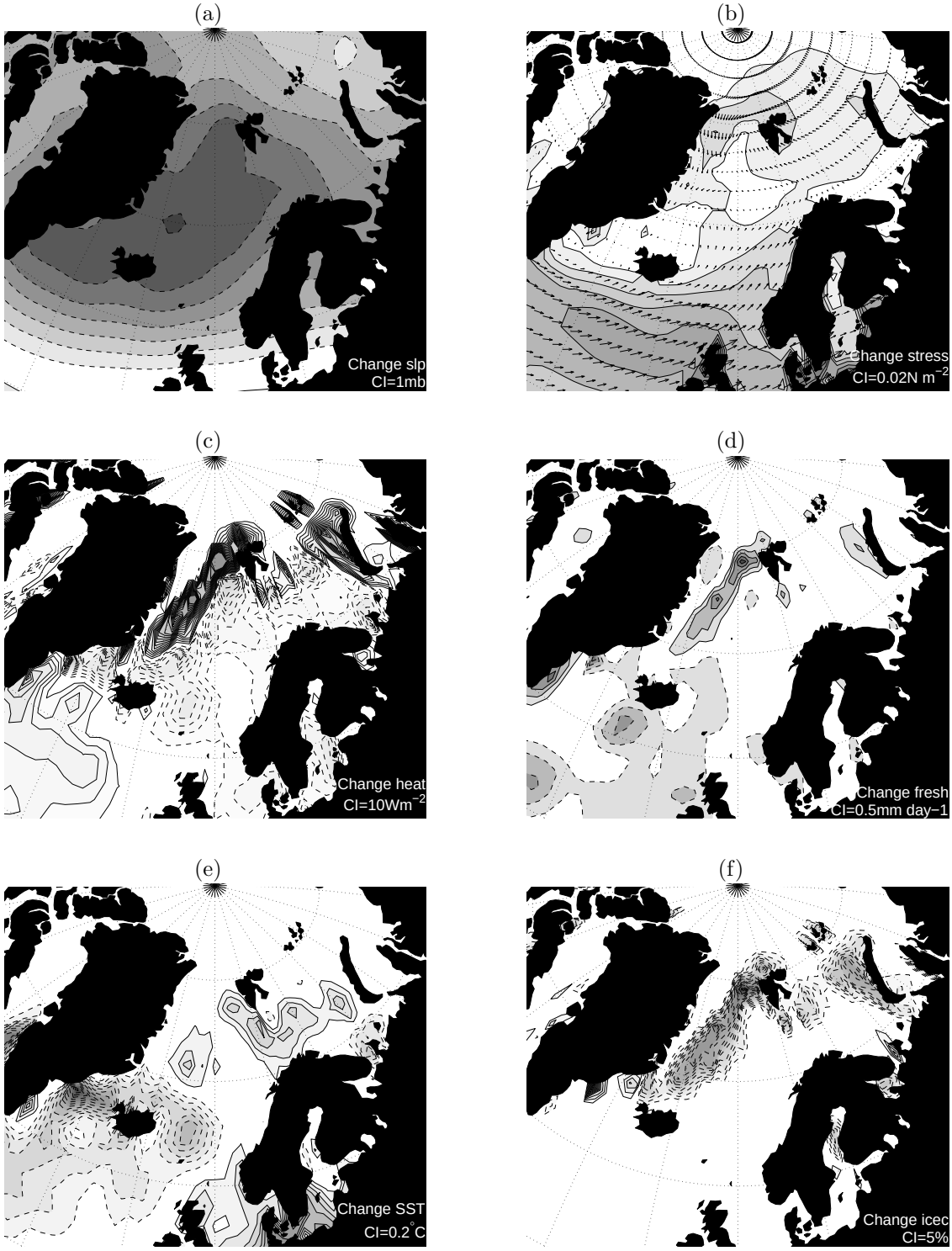

Figure 19. Change between the 15 years averages 1958–1972 and 1988–2002 for (a) SLP, (b) Wind stress, (c) Total heat flux, (d) Total freshwater flux, (e) SST, and (f) sea-ice concentration. Ekman transports of heat and freshwater (Figures 13 and 14) are not included in respectively (c) and (d). Solid lines are positive, dashed lines negative.